Master thesis

Master's degree of biomedicine

May 2021

Investigation of the expression profile of miRNAs regulating ADHD candidate genes.

William Akhtar

MABIO5900

60 Credits

Faculty of Health Sciences

OSLO METROPOLITAN UNIVERSITY
STORBYUNIVERSITETET

William Akhtar

Investigation of the expression profile of miRNAs regulating ADHD candidate genes

Master's degree Program of Biomedicine

Masteroppgave, 60 Sp

Faculty of Health Sciences

Department of Life Sciences and Health

OsloMet – Oslo Metropolitan University

Performed at

Norwegian Institute of Public Health

Division for Infection Control and Environmental Health

Section of Toxicology and Risk Assessment

Advisors

Nur Duale, Lene Brattsti Dypås, Gützkow, Kristine and Bjerve Olsen, Ann-Karin Hardie

Acknowledgment

The work presented in this master thesis was carried out at the Norwegian Institution of Public Health in the period from June 2020 to July 2021. Analysis of miRNA expression was performed at Division for Infection Control and Environmental Health, Section of Toxicology and Risk Assessment. My primary supervisor has been Dr. Nur Duale and Lene Brattsti Dypås MS, and Dr. Olsen, Ann-Karin Hardie and Dr. Gützkow, Kristine Bjerve ware co-advisor. I'm grateful to them for the opportunity to take my master's degree at their department.

Firstly, I want to thank both Nur and Lene for great advice and support. I'm thankful that they shared their experience and knowledge making my time at NIPH enjoyable as well as extremely informative. Secondly, I want to thank Dina Behmen and Jill Mari Andersen for showing and helping me with laboratory work. I also want to thank everyone at the department, for being included in a great and motivating environment. My time working at NIPH have given me great experience that I highly value and will cherish.

I want to show gratitude to my family and everyone whose encouraged and given me great support, it has been uplifting throughout my entire work as well making the process meaningful and enjoyable.

Abstract

Attention-deficit/hyperactivity disorder (ADHD) is the most common child-hood onset neuropsychological disorder, characterized by symptoms such as inattention and hyperactivity/impulsivity in varying severity across situations and over periods of time. It is thought that the symptoms derive from aberrant regulations of neurotransmitters, specifically, the catecholamines; Serotonin, norepinephrine and dopamine. Individuals effected by the disorder show difficulties in academical and social situation, as well as a higher likelihood of harmful outcomes such as substance abuse criminality, unemployment or other financial challenges. Poor understanding of ADHD`s ethology causes clinical assessment to be the best diagnostic tool, following the guidelines from International Classification of Diseases 11th revision (ICD-11) and Statistical Manual of Mental Disorders 4th edition (DSM-IV). ADHD`s prevalence is estimated to be 5-6% in youth, with one third of the youth carrying the disorder to adulthood. Twin studies have shown ADHD to be highly heritable, however it did not explain some of the heritability, this could prove epigenetic factors involvement.

miRNA is one epigenetic factor that has been shown potential for detecting ADHD. Firstly, it is well established that there is abundancy of miRNA in the central nervous system, and that they effect many aspects of neural development. Secondly, There are studies showing neuropsychological disorder ethology associated with aberrant miRNA function such as fragile X syndrome schizophrenia autism spectrum disorder (ASD) and Alzheimer disease(1);(2);(3);(4);(5);(6). Additionally, unlike mRNA, miRNA have been shown to be stable and freely circulating in biofluids, as well as in archived biofluids. These reports have been of importance for development of biomarkers derived from multiple fields such as cancer and tumour prognosis, lifestyle diseases and neurodegenerative diseases.

In this study, we evaluated the feasibility of using circulating miRNAs from blood plasma as biomarkers of ADHD. We investigated 1248 archived plasma samples gathered by MoBa, from umbilical cords of children, and blood from mothers and fathers. They consisted of 624 child-cord maternal and paternal plasma samples, where the child had in later life been clinically validated for ADHD according to the NPR diagnostics using ICD-10. The ADHD-case group would be compared with 624 cord maternal and paternal derived plasma samples, where the children were randomly selected non-ADHD participants that matched cases in age and gender.

Firstly, the plasma quality was assessed by screening multiple quality control parameters. Secondly, the analysis of miRNA expression of 16 miRNA, that has been reported to be targeting potential ADHD candidate genes. A Predictive model for identifying ADHD-cases was made using logistic regression on miRNA expression of the 16 relevant miRNAs.

There was a clear difference in discoloration between the cord samples then what was observed in maternal and paternal plasma sample. The spectrometric assessment showed child samples to be of low quality. Particle counts found paternal samples to contain more counts of both microparticle and platelets then child and mother had. There is clear evidence that the plasma quality used in this study is not optimal. There were no significantly different expressed miRNAs. However, two miRNAs were observed to be interesting, miR-125a-3p and miR-17-5p stood out from the remaining miRNAs both in comparing miRNA expression between ADHD-cases and control, and as a contributor for the predictive model.

Abstrakt

Attention-deficit/hyperactivity disorder (ADHD) er den vanligste nevropsykologiske forstyrrelsen ved barndom, preget av symptomer som uoppmerksomhet og hyperaktivitet/impulsivitet i varierende alvorlighetsgrad på tvers av situasjoner og over perioder. Det antas at symptomene stammer fra avvikende regulering av nevrotransmittere, spesielt katekolaminene; Serotonin, noradrenalin og dopamin. Personer som påvirkes av uorden viser vanskeligheter i akademiske og sosiale situasjonen, samt større sannsynlighet for skadelige utfall som rusmisbruk og arbeidsledighet eller andre økonomiske utfordringer.

Dårlig forståelse av ADHDs etologi fører til at klinisk vurdering er det beste diagnostiske verktøyet, hovedsakelig i henhold til retningslinjene fra International Classification of Diseases 11.revisjon (ICD-11) og Statistical Manual of Mental Disorders 4th edition (DSM-IV). ADHDs prevalens anslås til å være 5-6% hos ungdom, hvor en tredjedel av ungdommene bærer sykdommen til voksen alder. Tvillingstudier har vist at ADHD er svært arvelig, men noe av arveligheten ble ikke forklart, dette kan være bevise for involvering av epigenetiske faktorer.

miRNA er en epigenetisk faktor som har potensiale til å oppdage ADHD. Det er veletablert at det er overflod av miRNA i sentralnervesystemet, og at de påvirker mange aspekter av nevral utvikling. I tillegg er det studier som viser nevropsykologis lidelse etologi assosiert med avvikende miRNA-funksjon som fragil X-syndrom, schizofreni, autismespektrumforstyrrelse (ASD) og Alzheimers sykdom (1 38); (2 39); (3 40); (4 41); (5 42); (6 43). I tillegg har miRNA, i motsetning til mRNA, vist seg å være stabil og sirkulere fritt i biovæsker, så vel som i arkiverte biovæsker. Disse observasjonene har vært viktige for utviklingen av biomarkører avledet fra flere felt som kreft og tumorprognose, livsstilsykdommer og nevrodegenerative sykdommer.

I denne studien evaluerte vi muligheten for å bruke sirkulerende miRNA fra blodplasma som biomarkører for ADHD. Vi undersøkte 1248 arkiverte plasmaprøver samlet av MoBa fra navlestrenger til barn, og blodprøver fra mødre og fedre. De besto av 624 barn mødre og fedre, hvor barna ble klinisk validert for ADHD i henhold til NPR-diagnostikken ved bruk av ICD-10. ADHD-sak-gruppen ville bli sammenlignet med 624 barn mødre og fedre, hvor barna ble tilfeldig valgt ikke-ADHD-deltakere som samsvarte med tilfeller i alder og kjønn.

Første ble plasmakvaliteten vurdert ved å screene flere parametere for kvalitetskontroll. Deretter ble miRNA-ekspresjonen av 16 miRNA, som er rapportert å være komplimenter med

mulige ADHD-kandidatgener. En prediktiv modell for å identifisere ADHD-tilfeller ble laget ved hjelp av logistisk regresjon på miRNA-ekspresjon av de 16 relevante miRNAene.

Det var en klar forskjell i misfarging mellom barnas prøver enn det som ble observert i mor og fars plasmaprøve. Den spektrometriske vurderingen viste at barnas prøver var av lav kvalitet. Partikkelantall fant at fars prøver inneholdt flere tellinger av både mikropartikler og blodplater enn barn og mor hadde. Det er klare bevis for at plasmakvaliteten som brukes i denne studien ikke er gunstig. Det var ingen signifikant forskjellige uttrykte miRNAer, men to miRAN ble observert miR-125a-3p og miR-17-5p, de skilte seg ut fra de gjenværende miRNAene.

Abbreviations

MIRNA	Micro RNA
MOBA	The Norwegian Mother, Father and Child Cohort Study
NIPH	Norwegian institution of public health
ADHD	Attention-deficit/hyperactivity disorder
ICD-11	International Classification of Diseases 11th revision
DSM-IV	Statistical Manual of Mental Disorders 4th edition
PFC	Prefrontal cortex
CNS	Central nervous system
RNAI	RNA interference
MRES	miRNA response elements
UTR	Untranslated region
PRE-MIRNA	Precursor miRNA
PRI-MIRNA	Primary miRNA
POL II	RNA Polymerase II
DGCR8	DiGeorge Syndrome Critical Region 8
XPO5	Exportin 5
SHRNA	Short-hairpin RNA
AGO2	Argonaute2
AGO	Incorporated in Argonaut
MIRISC	miRNA-inducing silencing complex
POEMA	Potential Early Molecular Markers for ADHD
NPR	Norwegian Patient Registry
REK	Regional ethics committee
MP	Microparticle
LIH-SCORE	Lipemia independent Hemolysis Score
NA	Nucleic acids
RT	Reveres transcription
MIN	Minute
SEC	Second
MMLV HP RT	Murine leukemia virus high performance reverse transcriptase

PAP	poly(A) polymerase
R-PRIMER	Revers primer
F-PRIMER	Forward primer
TA	Annealing temperature
CQ	Quantitative cycles
RFU	Relative fluorescent units
ANOVA	One-way analysis of variance
AIC	Akaike`s information criterion
SE	Standard error
LIH-SCORE	Lipemia-independent Hemolysis score
NRQ	Normalized relative quantile
FC	Fold change
CBC	Complete blood count

Table of content

Introduction

The discovery of microRNAs (miRNA) as a crucial contributor for several biological processes (7), coupled with the observation that miRNA is stable and freely circulation in biofluids, highlighted the possibility of creating biomarkers based on miRNA derived from biofluids such as plasma, serum and whole blood. (8). Further, there have been found substantial evidence that aberrant miRNA levels are associated with neurological disorders (9), as well as cancer prognosis (10), thus, they are ideal as biomarkers (11). The advantage of using miRNA biomarkers that is derived from biofluids, is that it`s a less invasive method to facilitate early diagnosis and prognosis. The introduction of miRNAs as a diagnostic method to diagnose ADHD, have some promising features.

Firstly, biomarkers can replace clinical assessment to diagnose patients, mainly because clinical assessment rely on already developed symptoms. With biomarkers A patient could be screened for biological markers as soon as biofluids are available. Additionally, biological markers would report empirical data which further could be used for determining diagnosis, treatment and assessing severity of symptoms.

The development of empirical definitions for neuropsychological disorders such as ADHD, allows for proper investigation and comparisons of symptoms, response to treatments, and monitor disease progression. Biomarkers derived from biofluids such as plasma samples is a convenient source for both patient and researcher. The invasive properties of such sample collection allow from more systematic and regularly screenings. Most importantly, this makes it reasonable to investigate archived plasma samples collected in biobanks.

The Norwegian Mother, Father and Child Cohort Study (MoBa) is a prospective population-based pregnancy cohort study conducted by the NIPH. Participants were recruited from all over Norway from 1999 to 2008, and the cohort now includes more than 114,500 children, 95,200 mothers and 75,200 fathers (12). Biological material in the form of whole blood and plasma has been collected from the mother, the father and the child (umbilical cord blood) and stored in the Norwegian institution of public health`s Biobank, for future use (13).

To successfully discover miRNA-based biomarkers, the plasma quality should not be contaminated and should be of high quality. The main reason is that the number of miRNAs in plasma is so low and small contamination from preanalytical handling of the samples,

cellular leaked or hemolysis could alter miRNA levels greatly. Therefor analyzing plasma quality is essential when searching for novel miRNA biomarkers (14).

In this thesis, the predictive value of 16 selected miRNAs to distinguish between ADHD case and matched control will be evaluated. To do so, a plasma quality control protocol will be established in order to assess whether the plasma samples from MoBa biobank have an acceptable quality and can be used to find miRNA-based biomarkers of ADHD. miRNA biomarkers distinguishing between ADHD cases and matched controls can be used as an early diagnosis of ADHD. Identification of such predictive miRNA markers is of great significance for intervention, effective postnatal management, medical advancement and neurological understanding.

Attention deficient Hyperactive Disorder

Attention-deficit/hyperactivity disorder (ADHD) is the most common neuropsychological disorder, and it causes a dysfunction of the executive functioning through effecting neurotransmitter, mainly in the frontal lobes. This causes symptoms such as inattention and hyperactivity/impulsivity in varying severity across situations and over periods of time (15),(16). An extensive meta-analysis estimated ADHD`s prevalence to be 5-6% in youth (17).

Our limited understanding of ADHD`s ethology causes clinical assessment to be the main diagnostic tool, mainly following the guidelines from International Classification of Diseases 11th revision (ICD-11) and Statistical Manual of Mental Disorders 4th edition (DSM-IV) (17). However, the diagnostic methodology of ADHD is flawed, as there is a 2:1 ratio between the genders, a ratio that is not observed genetically, suggesting underdiagnosis of female ADHD patients. Additionally, ICD-11 and DSM-IV have different criteria for diagnosing ADHD, mainly revolving around methodology when observing ADHD`s characteristic traits: Inattention, Hyperactivity, and impulsivity (17).

Individuals are affected by ADHDs symptoms in varying degree and intensity; however, it is reported that ADHDs symptoms are associated with difficulties in academical and social situation (17), the result from loss of working memory and concentration. higher likelihood of harmful outcomes such as substance abuse (18) criminality (19) and mortality (20), and financial challenges such as unemployment (21). There are only 16% of adolescents that report outgrowing ADHD (22). Further 80% of adults with ADHD reported having at least one psychiatric disorder (23). Its hypothesised that as an individual gets older more of the

ADHD symptoms are internalized (24), resulting in multiple psychopathological illnesses, most commonly, ADHD is observed comorbid with bipolar depression anxiety mood and personality disorder(25, 26).

The ethology of ADHD is not completely understood, a twin study showed ADHD to be 70-80% heritable (27);(28). The fact that twins are not inheriting ADHD in all cases leads to some of the heritability not being explained. This could prove epigenetic factors being are being involved (29);(30);(31). There is extensive research done on the pathophysiology of ADHD. The prefrontal cortex (PFC) is central to the disorder, as it is the mediator of the cognitive functions that is impaired in ADHD patients (32).

ADHD is affecting the PFC through its neurotransmitter system, specifically, the catecholamines; serotonin dopamine and norepinephrine (33, 34). Most treatments used to cope with ADHD symptoms are targeting the catecholamines directly or indirectly through receptors inhibitors or promoters (35). These treatments have shown to be effective when used in early stages, as it eases the symptoms of ADHD and significantly reduces the risk of development of comorbid disorder (36)

Central nervous system

The central nervous system (CNS) is the complex system developed for processing and interpreting external stimuli, as well as being the coordinator of many voluntary and involuntary processes (37) These complex systems are developed from the vast neuronal network, and it is the transmission of endogenous chemicals between the neuron that allows for communication, resulting in our ability to think, communicate, experience emotions, develop new skills, and store information (37). The realisation that there is abundancy of miRNA in the CNS, as well as the growing field of neurodevelopmental disorders that has been associated with aberrant miRNA levels, highlights the important of understanding the interplay between miRNA, ADHD and CNS. There exists multiple neurotransmission-systems each having specific transmitters that allow for neurons to communicate. The different systems compose of varying amounts of neurons (38). Though catecholamines is only regarded as a small neural system, it is an important regulatory system of the neural network (33). The neurotransmitter monoamines, specifically catecholamines; serotonin, norepinephrine and dopamine are of great interest. These are transmitters that have overlapping functions such as alertness, attention, reward, motivation and anxiety, thus overall emotional regulation (33) (34).

In ADHD, it is been shown that catecholamines are dysregulated (39) it is also reported that the prefrontal cortex (PFC) and the visual cortex are regulated by these catecholamines, interestingly, the symptoms of ADHD derive from deficiencies in activity of these areas (39). It is believed that ADHD patients have a depleted level of these neurotransmitters, and that this is caused by aberrant catecholamine transport, resulting in inattention, hyperactivity, and impulsivity (33) (32) (34). Naturally the therapeutic treatments, most commonly methylphenidate and amphetamines (40), target these catecholamine transporters to compensate for the depleted levels of the neurotransmitter (41). The mechanism behind these therapeutic drugs aim to increasing the availability of dopamine and norepinephrine, by decreasing the reuptake of the neurotransmitter, through inhibiting the dopamine and norepinephrine transporters (41).

microRNAs

MicroRNAs (miRNAs) are a class of short non-coding RNAs of ~ 22 nucleotide in length that play important roles in regulating gene expression. Their role in gene regulation was first identified in *Caenorhabditis elegans* in the early 1990s, when Lee and Finebaum observed the lin-4 nucleic acid and identified its function in *Caenorhabditis elegans* larva development (42). They found that lin-4 synthesised antisense RNAs consisting of 22-61 nucleotides, some of which were complimentary to lin-14 mRNA and would inhibit further protein synthesis. They concluded that there were small RNA mediated mechanisms that interfered with mRNA. However, this function was at the time thought to be a Nematode idiosyncrasy.

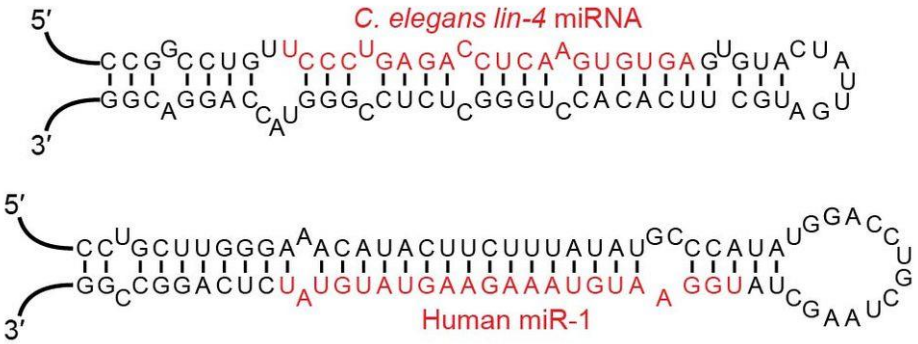

Figure 1: lin-4 miRNA illustrated to show the characteristic structure of miRNA, as well as similarity's with humane miRNA. Examples of microRNA stem-loops, created by VTD, CC BY-SA 4.0.

Later in the early 2000s the concept behind miRNAs became refined, as the small let-7 RNA was observed to be both, related to lin-4, and conserved in human-cells (43, 44). These advances led to the discovery of RNA interference (RNAi) which awarded Fier and Mello the

Nobel Prize in physiology or medicine in 2006, and thus the important role of miRNAs was made clear (45).

miRNAs were found to origin from DNA transcripts, and most miRNAs were found to be transcribed from introns, but it is reported to derive in exons as well (46). They target approximately 60% of mRNA, largely because of the conservation of miRNA response elements (MREs) residing in the 3`-untranslated region (UTR) of mRNA (47). They show similar regulatory effect as hormones, since extracellular miRNAs regulate cells autocrine, paracrine and endocrine (48). The total number of miRNA present in a human cell is not yet clear, some strict studies suggesting the miRNA number found in a human cell to be around 600 miRNAs (49). However, newer studies estimated around 2300 miRNAs in a human cell (50), The exact number of miRNAs is hard to estimate because of the wide variety of miRNAs that derive from precursor miRNA (pre-miRNA) (51). In the miRBase database (http://www.mirbase.org), there are currently around 2 500 annotated mature miRNAs from humans.

miRNA biogenesis and their mechanism of action

miRNAs biogenesis and mechanism utilize two main types of pathways, either canonical or non-canonical. These pathways both produce pre-miRNA, however the difference is that canonical predecessor is genome derived, and in the non-canonical pathways there are multiple predecessor molecules, which derives from different sources. The pathways utilize similar enzymes for maturation but in different combinations based on the predecessor molecule. The non-canonical pathways could be further separated by what combinations of maturation enzyme needed. After maturation, pre-miRNA is exported out of nucleus (52).

Canonical pathway: In this pathway the predecessor molecule is called primary miRNA (pri-miRNA) and is genome derived. Pri-miRNA is translated from DNA by RNA Polymerase II (pol II), further the dsRNA-binding-protein DiGeorge Syndrome Critical Region 8 (DGCR8) recognise and binds the motifs of pri-miRNA (53). The bound pri-miRNA is cleaved at its 5`and 3`end by Drosha a RNase III enzyme, resulting in pre-miRNA. Pre-miRNA is further exported out of nucleus by exportin 5 (XPO5) (54).

Non-canonical pathway: In this pathway the predecessor molecules come from many sources, and there are multiple different pathways, mainly separated by what combination of canonical pathway enzymes they utilize. Some examples are mirtron, that is derived from introns of mRNAs during splicing, which is directly exported out of nucleus by XPO5. Also, short-

hairpin RNA (shRNA) is a predecessor for pre-miRNA that utilizes a different non-canonical pathway. similarly, to pri-miRNA it is matured to pre-miRNA by the enzymes DGCR8 and Drosha and exported to cytosol by XPO5.

Additional processing of pre-miRNA in cytosol is necessary (52). pre-miRNA derived from mirtron and pri-miRNA is processed by the RNase III endonuclease Dicer, Dicer cleaves the terminal loop, resulting in a mature miRNA with imperfect duplex, consisting of a guide strand and a passenger strand ((55), (54),(56)). The pre-miRNA derived from shRNA is processed differently, as additional cleavage by Argonaute2 (AGO2) in the cytosol is necessary. Finally, the miRNA`s guide strand, which is either the 5p or 3p strand, is incorporated in Argonaut (AGO) to form a miRNA-inducing silencing complex (miRISC) (57).

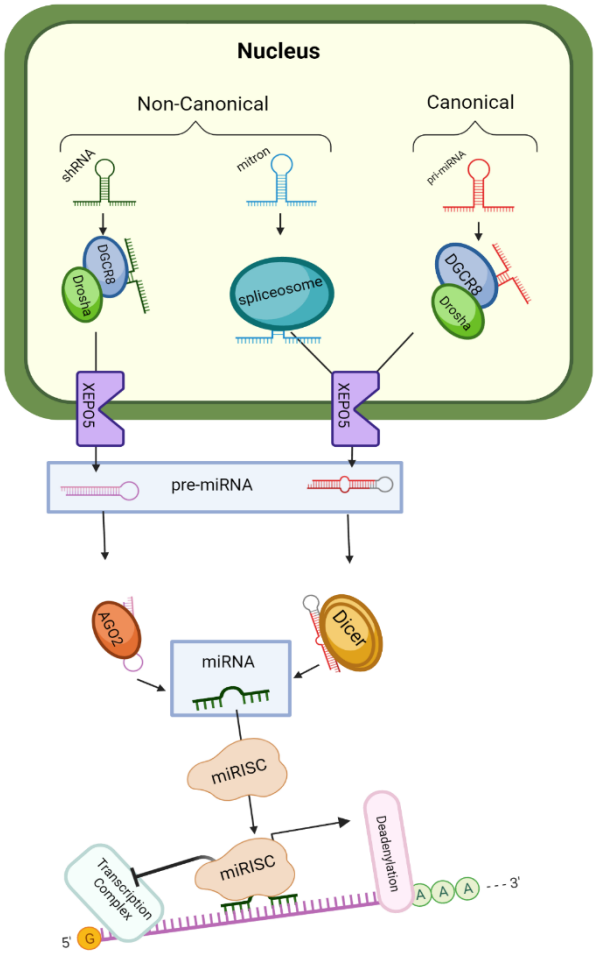

Figure 2: shows the miRNA biogenesis pathways of both Canonical and non-canonical Created with BioRender.com. the miRNA biogenesis is divided into two pathways; canonical and non-canonical. Pre-miRNA is matured to miRNA by removal of the loop, further the guide strand, either 5p or 3p, is incorporated to miRISC complex. miRISC complex preformed gene silencing in animals by inhibiting translation, as well as deadenylating of the poly(A) tail. Resulting in degraded of mRNA. Created with BioRender.com

Although MRE is thought to reside within the 3` UTR, there are findings that miRNA also have targets in the 5`UTR, as well as interactions with promotors. The binding of miRNA in 5`UTR has shown to have silencing effects, but interestingly miRNA binding with promotors have shown to induce transcription (58). The degree of complementary in the miRNA-MRE interaction, dictates the activity of AGO2`s endonuclease cleavage therefore, either inhibition or degradation of mRNA is performed ((59, 60)). In animal cells most of the MRE-miRNA interaction induces miRISC inhibition and not degradation, because of the improper structure of the miRNAs (Figure 2) binding of miRNA-MRE is not ideal for AGO2 endonuclease binding (61). miRISC mediated inhibition revolves around multiple enzymes, resulting in two mechanisms. Firstly, the miRNA-MER interaction has shown to inhibit translation of mRNA, secondly, deadenylates of poly(A) tail, causing the mRNA to destabilize, eventually resulting in degradation (61) (Figure 2).

Circulating miRNAs roles

There are extensive reports of miRNAs release, and presence in biofluids. Contrary to mRNA, extracellular circulating miRNAs are highly stable and resistant to degradation (62). There are different types of extracellular miRNAs, protein-coupled miRNA (63) and membrane bound miRNA derived vesicles such as exosomes micro vesicles and apoptotic bodies ((64), (48)). These two sources of miRNA are not yet fully understood, as there is discrepancy in which`s the relevant source of miRNA, and whether these sources are of equal importance as biomarkers (61). miRNAs role in multiple aspects of cell function as well as its, stable presence in biofluids made it ideal as a source of biomarkers. There are now well-known biomarkers derived from multiple fields such as cancer and tumour prognosis, lifestyle diseases like cardiovascular disease and diabetes, viral infections and neurodegenerative diseases such as fragile X syndrome, schizophrenia, autism spectrum disorder (ASD) and Alzheimer disease(1);(2);(3);(4);(5);(6).(9).

AIM of study

The overall aim of this master thesis is to investigate whether the expression levels of some selected miRNAs in plasma samples from ADHD cases differ significantly from age and gender matched controls. The miRNAs selected are potential targets for ADHD candidate genes. Our aims were:

- Evaluate the feasibility of plasma samples isolated from cord, mothers and fathers stored at MoBa biobank can be used to identify miRNAs marker distinguishing ADHD cases from matched controls.
- Identify difference in expression of ADHD-targeting miRNAs between ADHD-cases and matched control in plasma samples.

Method

MoBa

The study is a part of the Potential Early Molecular Markers for ADHD (POEMA), the main goal is to contribute to early detection and prevention of ADHD. Linked with the MoBa-project with extensive information of subject lifestyle and environment exposure from child, mother and father, and the Norwegian Patient Registry (NPR) with clinical validated records of subjects diagnosed with ADHD. The analysis of epigenetic modification (circulating-miRNA and DNA-Methylation), environment exposure and lifestyle, across mother, father, child is done to investigate to find potential these markers. This was a nested case-control project/study using the resources from MoBa, a sample size of 1248 participants, consisting of 624 clinically validated ADHD cases according to the NPR diagnostics using ICD-10, and was compared with 624 randomly selected non-ADHD MoBa participants, that matched cases in age and gender.

Ethics

The biological samples used in this project was gathered and stored in the MoBa biobank. The participants from the MoBa-Project gave broad consent for using the samples and, de-identified health information for research. According to the committee, this consent, covers the goal of the study, and the project`s focus does not include Whole genome or exosome sequencing. The Regional Ethics Committee and the Data Inspectorate approved the MoBa study, and participants gave their informed consent. The regional ethics committee (REK) and the NPR have approved the POEMA project. This thesis is a sub-part of the POEMA project.

Blood plasma extraction

Maternal and paternal blood samples used in this project were collected at gestational week 17-19, and umbilical cord vein blood were collected at delivery. Blood plasma was extracted from blood samples collected in EDTA-tubes. The EDTA-tubes containing whole blood were centrifuged at 1508 g for 10 minutes for 5 min at room temperature and plasma carefully removed into a separate tube away from any residual debris. A 6 x 300µl aliquot of the extracted plasma sample from each subject were pipetted into a microtiter plates with barcode and stored at -80°C. Maternal and paternal plasma were extracted at maternity units or at the hospital before shipping to NIPH. While Umbilical cord blood were sent to the MoBa Biobank for processing.

Quality control of Plasma Samples

The maternity units or hospitals where blood sample collection took place are located all over Norway, and from a few hours up to several days may be required before the blood samples arrive for processing at the NIPH biobank. The preanalytical sample handling parameters such as distance between blood collection location and the biobank, and the associated differences in duration and temperature fluctuations during transportation, may affect the quality of the obtained blood plasma and subsequently the miRNA expression data. Further, plasma samples may contain residual proteins or other contaminants that may inhibit or affect downstream analysis. Therefore, an assessment of the quality of the plasma samples should be determined.

When studying circulating-miRNAs in plasma sample, a well-known contamination source is endogenous components. The biggest source of contamination is from haemolysis of erythrocytes, haemolysis would compromise the quality of the exogenous circulating-miRNA (65). The degree of haemolysis can be estimated in several ways. In this study three different method was used; I) A visual estimation of plasma discoloration caused by the release of oxyhaemoglobin enriched in erythrocytes. II) A Spectrophotometric analysis (Nanodrop) of the optical density from the plasma sample, capable of detecting oxyhaemoglobin and quantifying it. III) A miRNA expression analysis where miRNA known to be enriched in erythrocytes would be compared with miRNA known to be stably present in plasma.

The presence of platelets and micro particles (MP`s) has been shown to be abundant when investigating archived plasma and is confounding the measurement of extracellular miRNA (66). During blood plasma extraction, additional centrifugation was done to remove platelets in plasma. Though additional steps to remove platelets was done, there is evidence showing increase in residual platelets and MP`s in plasma that has undergone freeze/thaw cycles. Therefore, quantifying platelets is necessary for a complete assessment of plasma quality. In this study the residuals were measured using electric current exclusion (CASY), detecting particles and estimating its size.

Detection of plasma microparticles using Casy instrument

To detect residual Blood platelets and MP`s the highly accurate multi-parameter CASY cell analyser (Roche, Norway) was used, utilising an electric current exclusion technology also known as Coulter principle. Diluting samples in a conductive isotonic buffer, would create a constant current of 1MHz voltage. particles crossing this current makes it fluctuate, the degree to which the current is disrupted corresponds to the particles size (Range=0,7-45µdm). Thus, using the CASY cell analyser the presence of residuals platelet would be detected at the diameter range 2-5µdm and microparticles at ≤1,5µdm (67) (Figure 3). The expected counts range of residual platelet in non-treated whole blood is 1,5-4,5x10^5 µL/L

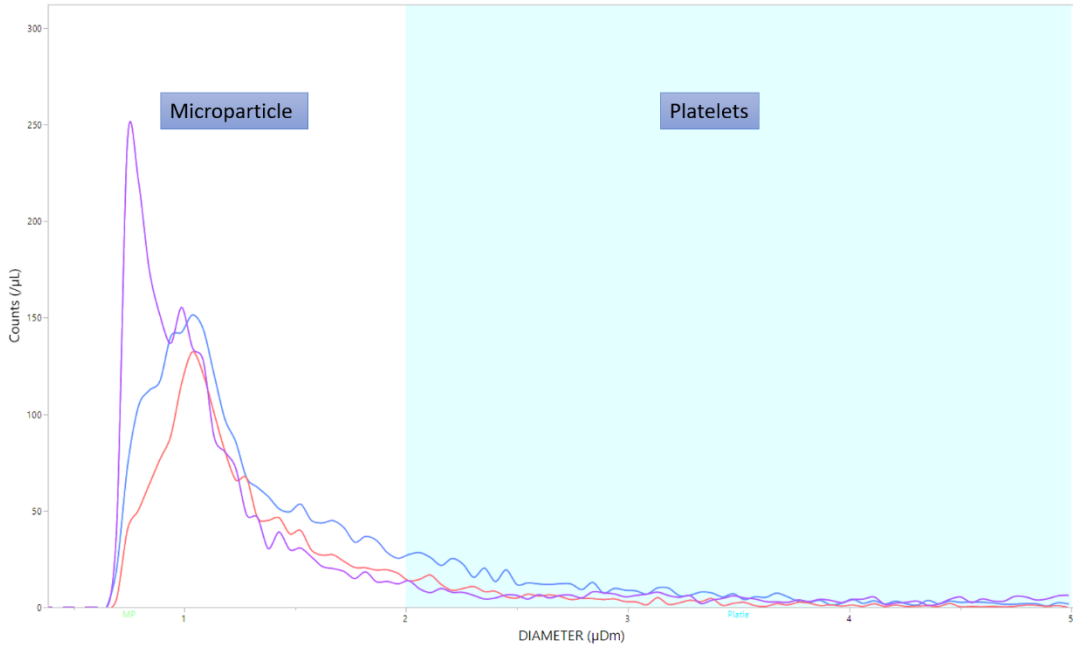

Figure 3: three measurement of plasma samples with different degree of hemolysis. Showing Intervals of expected micro diameter for MP`s (clear) and platelets (blue).

Measuring potential contaminations in the plasma samples less than 5µm in diameter was done using the CASY cell counter and Analyzer Model TT (Roche/OMNI Life Science, United Kingdoms). First 3µL aliquoted plasma samples thawed for 1 hour at 8°C was diluted 1:2000 with 6mL pre-2µm vacuum filtered CASYton (OMNI Life Science, Cat: 5651808) in a CASYcup (OMNI Life Science, Cat: 5651794). Then a 45µL pore size capillary was washed for two cycles with 400µL of three different 10mL CASYcups contenting 10mL of CASYclean (OMNI Life Science, Cat: 5651787), 10mL RNase-free water and 10mL filterd CASYton. Casy cell counter then measured 200 µL of the sample twice and the mean was reported.

Plasma haemolysis assessment

Visual assessment

Visual assessment of haemolysis is possible but not quantifiable, therefore, each plasma sample was individually graded; 0; 1; 2 and 3 shown in Figure 4. 0 being clear indicating less haemolysed and each subsequently category describing an increasing in discoloration and haemolyses. This visual score is a guide that will be used along with the other haemolysis assessments to establish correlation between a visual estimation and quantitative data.

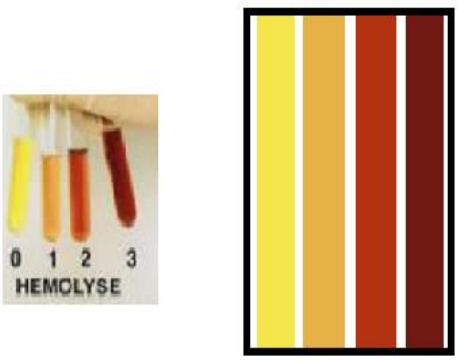

Figure 4: The reference template used to determine grading level of collected plasma samples.

Nanodrop/detection of oxyhaemoglobin using spectrometry

Nanodrop is a commonly used instrument that gives robust results with low preparation time and sample consumption. Oxyhemoglobin is detectable with nanodrop as peaks at 414nm (oxyhemoglobin) and 541nm, 576nm (deoxyhemoglobin) wavelengths (Figure 5). The absorbance rate where 414nm>0,2 would be defined as hemolyzed (Figure 5) (65). It is been shown that translucency increases the detected absorbance rate of a sample. The main source of translucency comes from lipemia, Thus, a lipemia-independent Hemolysis Score (LIH-Score) should be calculated. Since the absorbance at 385nm correlates with lipemia interference, a function could be made (function 1)

$$HS = \Delta_{A414-A385} + 0{,}16 * A385 \quad (1)$$

Hemolysis score, as a sum of the difference between absorbance of 414nm and 385nm($\Delta_{A414-A385}$), and the product of absorbance at 385nm and the angular correlation coefficient (-0,16) as a correction factor(68). A threshold for identifying hemolysis was calculated, from to be the sum of mean LIHS-score, and 3 standard deviation of the mean (Figure 5).

Using the Nanodrop™ 1000 UV-VIS spectrometry (Fisher Scientific, Norway) an Ultraviolet-visible spectrometry across the 220-700nm wavelength was done on 2µL aliquoted plasma

samples; thawed for 30 min at 8°C. RNase-free water was used to both clean the sample pedestal (5µL) and as a blank (2µL). Between each sample measurement the pedestal was cleaned and dried using RNase-free water and lint-free tissue.

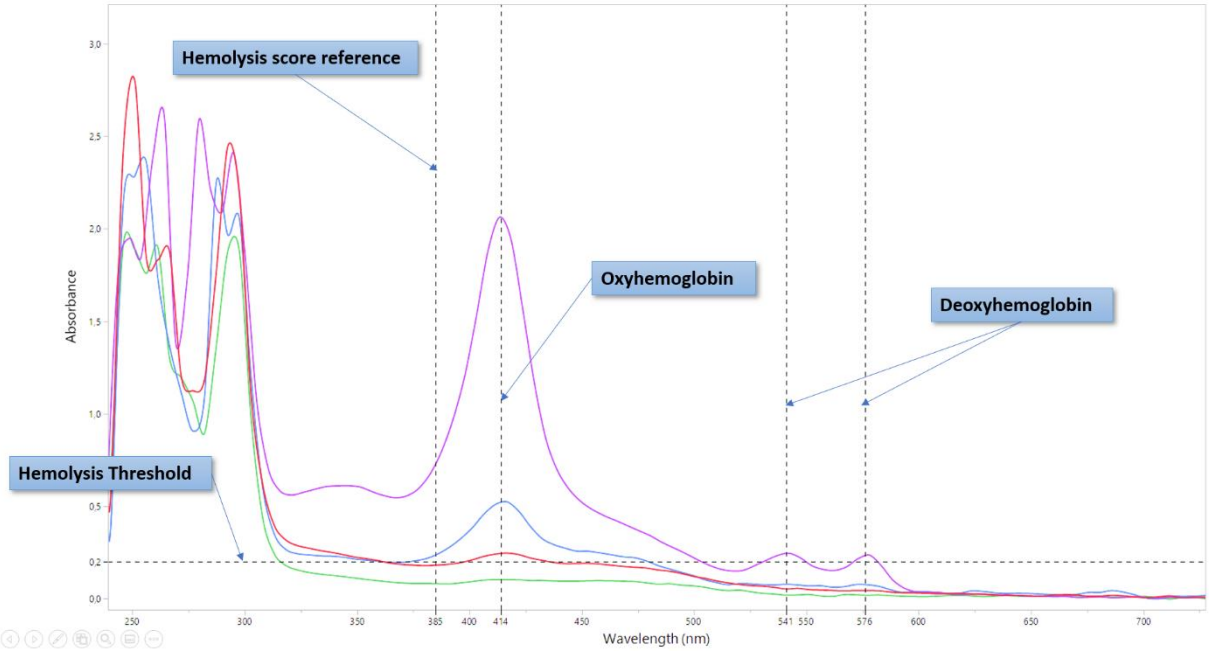

Figure 5: The graph illustrates four different degrees of hemolysis of plasma samples, green=1, Red=2, blue=3 and purple=3. The threshold used for determining hemolysis was set to 0,2 absorbance at wavelength of oxyhemoglobin (414nm). The graph also shows what wavelength was used to calculate hemolysis score, and detection of Deoxyheamoglobin (541 and 576nm).

QPCR Detection of erythrocyte enriched miRNA

The haemolysis assessment method previously explained, mainly focus on detecting and quantifying the degree of haemolysis. Ether indirectly (Visual assessment) or directly (Nanodrop). This method is an indirectly method of detecting haemolysis, it's based on comparing quantification cycles (C_q), using quantitative polymerase reactions.

The degree of haemolysis correlates with the presence of has-miR-451, a miRNA known to be enriched in erythrocytes (14). Comparing the C_q value of has-miR-451 with has-miR-23a, a miRNA known to be stably expressed in plasma. This method will directly measure miRNA contamination in plasma samples. The difference in expression, given as quantification cycles (C_q), was calculated using function 2:

$$\Delta C_q = \mathrm{C_{q(23a)}} - \mathrm{C_{q(451)}} \qquad (2)$$

ΔC_q determines the degree of haemolysis. A value below five would be an indication of pure samples, above five gives reason to suspect contamination, and values between 7-8 would confirm contamination. (14).

Plasma RNA Isolation

To further analyse the relevant miRNA, total RNA needs to be extracted and purified from plasma samples. Using the MagMax mirVana total RNA isolation kit (Cat. no. A27828, Fisher Scientific) with KingFisher™ Flex Magnetic Particle Processor 96DW (Cat. no. 5400630, Thermo Scientific) according to manufacturer's protocol. In brief, the kit would utilize coated paramagnetic beads, to reversibly bind total nucleic acids (NA) to the bead, creating NA-bead complex. In this study MagMAX™ magnetic beads was used, its coated with a bio-reactive polymer, like silica and has a strong affinity to NA under chaotropic conditions. The superparamagnetic properties of the magnetic bead make it possible to repeatedly extract and deposit total NA (Figure 6).

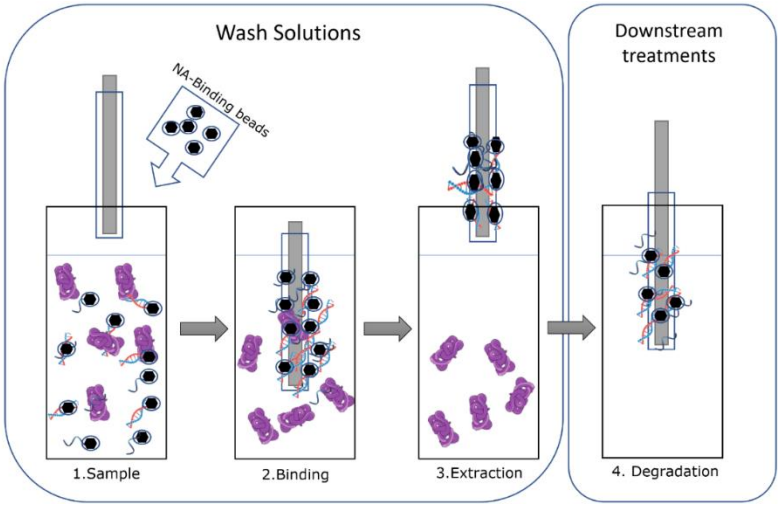

Figure 6*: illustrates the basics behind MagMax mirVana total RNA isolation kit principle. The magnetic rod (grey) covered by the tip comb (Blue line). With a solution containing DNA, RNA, binding-beads(yellow) and proteins.* ***Step 1*** *(sample) shows a coated magnetic bead binding to NA creating a bead-NA complex.* ***Step 2 (****binding) shows the bead-NA complex binding to a magnetic rod.* ***Step 3 (****Extraction) The magnetically bound bead-NA complex being easily removed from sample matrix.* ***Step 4 (****downstream Treatment) illustrates the simplicity of treating samples, when bound to a magnetic rod. In this case the NA-bound proteins are washed from NA-Bead complex. Alternatively, the rod could be placed in DNase to digest DNA, leaving only RNA-Bead complexes left.*

Using KingFisher™ Flex Magnetic Particle Processor, the NA-bead complex was processed with seven prepared plates containing buffers to purify total RNA; four washing plates for the removal of NA-bound proteins and salts; a DNase plate to degrade bound DNA; a elution plate, containing a buffer optimal for separating bound NA from NA-bead complex

Spike-in con

As a spike-in control for assessing the miRNA yield after isolation as well as being used for normalisation of miRNA expression, a known concentration of pooled cel-mIR-39, cel-mIR-54 and cel-mIR-238 was made. By mixing 10µL of each cel-miR-miRNA 10µM and diluting it to 5pM with RNase-free water Pooed cel-miR was made. Pooled cel-miR was placed on ice and added to the sample plate after the incubation of proteinase k step (table 1).

Processing plates Preparation

Seven MagMAX™ Express-96 Deep Well Plates (Cat. no. 4388476, Thermo Scientific) for processing NA-bead complex ware prepared shown in table 1. Solutions ware transferred to the plates using Integra Reagens-reaservoir (Cat: 613-3194, VWR) and multichannel pipette (Cat: 732-1434, VWR), and plates were sealed and stored on ice until used.

1. **The sample plate** was prepared with 100µL plasma transferred to a MagMAX™ Express-96 Deep Well Plates (Cat. no. 4388476, Thermo Scientific). Then 5µL proteinase K and 45µL PK digestion buffer was added to degrade proteins and mixed with on a Thermo Scientific™ Compact Digital Microplate Shaker (Cat. no. 11-676-337, Fisher Scientific) for 5 minutes at 1050rpm followed by inactivation of proteinase K by incubation for 30 minutes at 65°C.
2. Four plates **Wash Plates** were prepared to contain was solutions. Wash solution 1 and 2 was diluted in respectively 10mL isopropanol and 48 mL ethanol. 150µL wash solution 1 was transferred to one MagMAX™ Express-96 Deep Well Plates (Cat. no. 4388476, Thermo Scientific) and 150µL wash solution 2 to the three remaining plates.
3. A **DNase plate** for degrading DNA was prepared by mixing 48 µL MagMAX™ TURBO DNase™ Buffer with 2 µL TURBO DNase™ before carefully being vortexed transferred to a MagMAX™ Express-96 Deep Well Plates (Cat. no. 4388476, Thermo Scientific) then sealed.
4. The **elution plate** was made by transferring 50 µL Elution Buffer to a MagMAX™ Express-96 Deep Well Plate (Cat. no. 4388476, Thermo Scientific) and sealed.

*Table 1: showing plates made and reagents added (µL) for the KingFisher™ Flex Magnetic Particle Processor 96DW (Cat. no. 5400630, Thermo Scientific), coupled wash plate 2-4 since they are identical. Rebinding buffer and isopropanol was added to the DNase plate manually (*the plate was removed and treated with rebinding solution).*

	Reagent	**volume (µL)**
Sample Plate	**Plasma**	**100**
	Proteinase K mix:	**50**
	Proteinase k	5
	PK digestion buffer	45
	Lysis/Binding Mix:	**100**
	Lysis/Binding Enhancer	99
	2-Metacaptoethanol	1
	RNA Binding Beads	**20**
	Isopropanol	**270**
Wash plate 1	**Wash solution 1**	**150**
	Isopropanol	
	Wash 1	
Wash plate 2-4	**Wash Solution 2**	**150**
	Ethanol	
	Wash 2	
DNase Plate	**DNase Solution**	**50**
	DNase	
	MagMAX™ TURBO DNase™	
	Buffer	
	Rebinding Buffer*	**50**
	Isopropanol	**100**
Elution Plate	Elution Buffer	**50**
Tip Comb	MagMAX™ Express-96 Deep Well Tip Combs (Cat. no. 4388487)	8stk

Extraction

Firstly, Lysis/binding mix was made by diluting 1µL 2-mercaptetahnol in 99µL lysis buffer and mixed by pipette. Then 5µL proteinase K and 45µL PK digestion buffer was added to degrade proteins and mixed with on a Thermo Scientific™ Compact Digital Microplate Shaker (Cat. no. 11-676-337, Fisher Scientific) for 5 minutes at 1050rpm followed by inactivation of proteinase K by incubation for 30 minutes at 65°C.

Second 100µL of lysis/binding mix and 20µL RNA binding beads was transferred to the sample plate and mixed using Thermo Scientific™ Compact Digital Microplate Shaker (Cat.

no. 11-676-337, Fisher Scientific) for 5 minutes at 1050rpm in 22°C. Then 270µL isopropanol was added and the sample plate was mixed with Thermo Scientific™ Compact Digital Microplate Shaker (Cat. no. 11-676-337, Fisher Scientific) for 10 seconds at 1050rpm in 22°C.

All the prepared processing plates were placed in the KingFisher™ Flex Magnetic Particle Processor 96DW (Cat. no. 5400630, Thermo Scientific) as instructed by the software protocol A27828_Flex-BioFluids shown in. The plates were placed in the plate loader as shown in included with KingFisher™ 96 Tip Comb for DW Magnets (Cat. no. 97002534, Thermo Scientific).

After the system had DNase treated the samples, the DNase plate then containing the samples total RNA were taken out and treated with 50µL rebinding buffer and 100µL isopropanol and placed back into the KingFisher™ Flex Magnetic Particle Processor (Cat. no. 5400630, Thermo Scientific) and resumed protocol. When the KingFisher™ Flex Magnetic Particle Processor 96DW (Cat. no. 5400630, Thermo Scientific) had executed the protocol, 8µL of each well from the elution plate was aliquoted, sealed and stored at -80°C.

Quantifying plasma RNA concentration

Quantification of the isolated RNA yield is very important for miRNA expression profile analysis. Although quantifying RNA usually is done with Nanodrop, Qbit or Bioanalyzer, these methods limit of detection is up to 10-fold above the expected concentration of circulating RNA (Figure 7). 4,9µL Isolated RNA was therefore quantified using Low Abundance RNA Quantification Kit, a method which is more comprehensive but has the higher sensitivity needed to detect RNA at the low end of pg/µL.

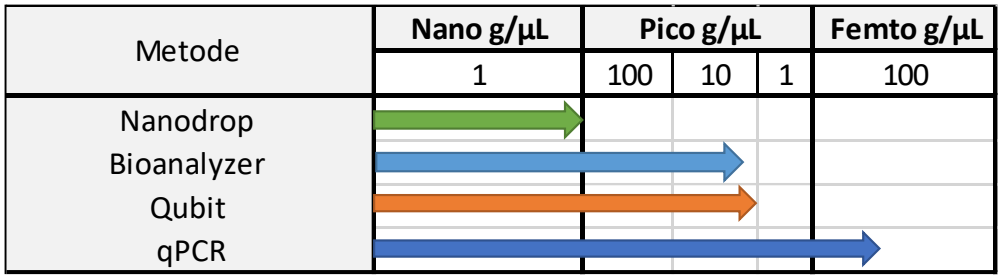

Figure 7: A illustration showing the range some of the most standard quantification methods and their limit of detection.

Plasma RNA yield was measured using Low Abundance RNA Quantification Kit (Norgen, Cat# 58900) according to the manufacturers protocol with a modification. In brief, a 5-point standard curve, made from a dilution series ranging from 100ng/µL-500fg/µL (Figure 8) was made. A regression function could be made where the Cq-value would be a function of RNA concentration, the quantitative relation between sample and standard RNA is equal to the volume of each RNA used.

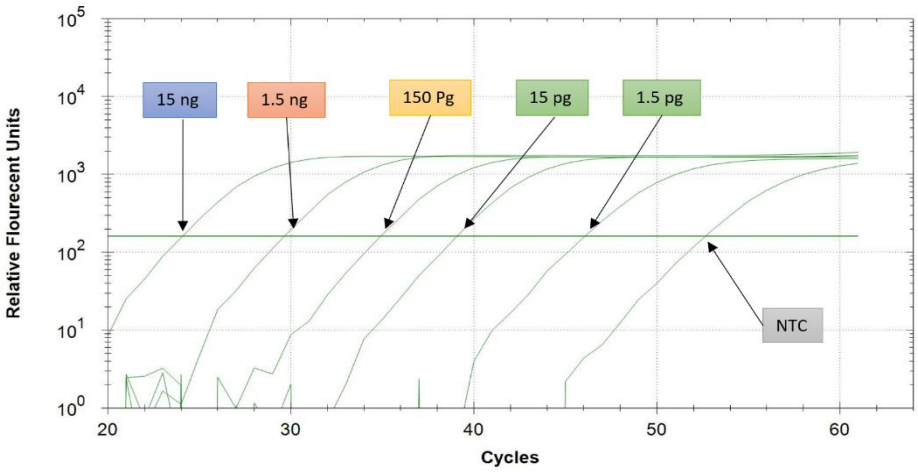

Figure 8: The dilution series used to create a standard curve where the Cq-value of a given dilution. Measuring samples and comparing reported Cq-value with the standard to approximate RNA yield.

Plasma RNA concentration measurement by qPCR.

First the revers transcription (RT) of both sample RNA and RNA standards were done, to synthesise a thermal stable cDNA. A master mixes (table 2 RT) containing 5µL 2x micr o Script Reverse transcription Master Mix, 0,5 µL MicroScript microRNA Enzyme Mix, 1µL RNA standard or 4,9µL RNA sample was made. Then the reaction was placed on a thermal cycler with the cycles shown in table 3.

Table 2: shows components (µL) used to separately synthesize cDNA from template RNA, sample RNA was isolated from Plasma sample, standard RNA was delivered by distributer.

	Component	Volume (µL)
RT	2x microScript Reverse Transcription Mix	5
	microScript miRNA Enzyme Mix	0,5
	RNA (standard or sample) *	1 or 4,9
	Nuclease-Free Water	3,5 or 0
	Total Volume	10
qPCR	2x Real-Time PCR Master mix	10
	RNA Quantification Primer Mix	2
	cDNA (standard or sample) *	2,5
	Nuclease-Free Water	5,5
	Total Volume	20

Second a qPCR Run was done by making an Master mix (table 2 PCR) with a reaction volume of 20µL consisting of 10µL 2xReal-Time PCR Master Mix, 2µL RNA quantification primer mix and 2 µL cDNA sample or standard, the samples were placed in an Real-time QPCR and with the cycles shown in table 3.

Table 3: Shows the Thermal Cyclers settings for both Revers transcription, and for qPCR.

	Cycle	Step	Cycles (°C)	Time (min)
RT	1	Hybridisation	37	30
		Extension	50	30
		Inactivation	70	15
		Hold	4	Hold
				Time (sec)
qPCR	1	Activation	95	180
	40	Denaturation	94	15
		hybridization	60	30
		elongation	72	45

miRNA expression level analysis by qPCR

The expression profile of miRNAs (n =16) selected based on recent report (69) were analyzed by Real-time (qPCR) assay. QPCR is considered a “golden standard” for gene expression analysis because of its specificity. QPCR Analysis performed with RNA requires additional handling to increase thermal stability, improve primer options and enriching the samples (Figure 9).

Since the RNA would be degraded under the temperatures induced by real-time qPCR, it is necessary to revers transcribe sample RNA to cDNA, additionally to improve specificity of primer hybridization, a poly(A) tail would be added. Since there are similar conditions set for poly(A) tailing and revers transcription, both methods could be coupled in one thermal cycler, thus, as the poly(A) tail would be added to the miRNA, it would consecutively be revers transcribed to cDNA. A Master mix containing both Murine leukemia virus high performance reverse transcriptase (MMLV HP RT) and poly(A) polymerase (PAP) would be added with the templets and placed on a thermal cycler.

Because of the poor yield of total RNA from plasma samples, the cDNA would not be enough to study all the candidate miRNA (n=17). Therefore, After the synthesis the cDNA contain identical sequence at the 5`end of the all cDNA its efficient to use this as a universal revers primer (R-primer). Coupling the R-primer with a miRNA specific forward primer (F-Primer), only the miRNA of interest would be amplified to sufficiently investigate candidate miRNA.

After the samples was prepared by Poly(A)tail, revers transcribed, and amplified the miRNA expression would be done using real-time qPCR. Real-time qPCR much like PCR would amplify the samples by treating them with different temperatures results in polymerase reactions. Contrary to PCR the real-time qPCR product would after each cycle be detect by fluorescent intensity from a DNA binding fluorophore. Fluorescent intensity is relative to amount of qPCR product.

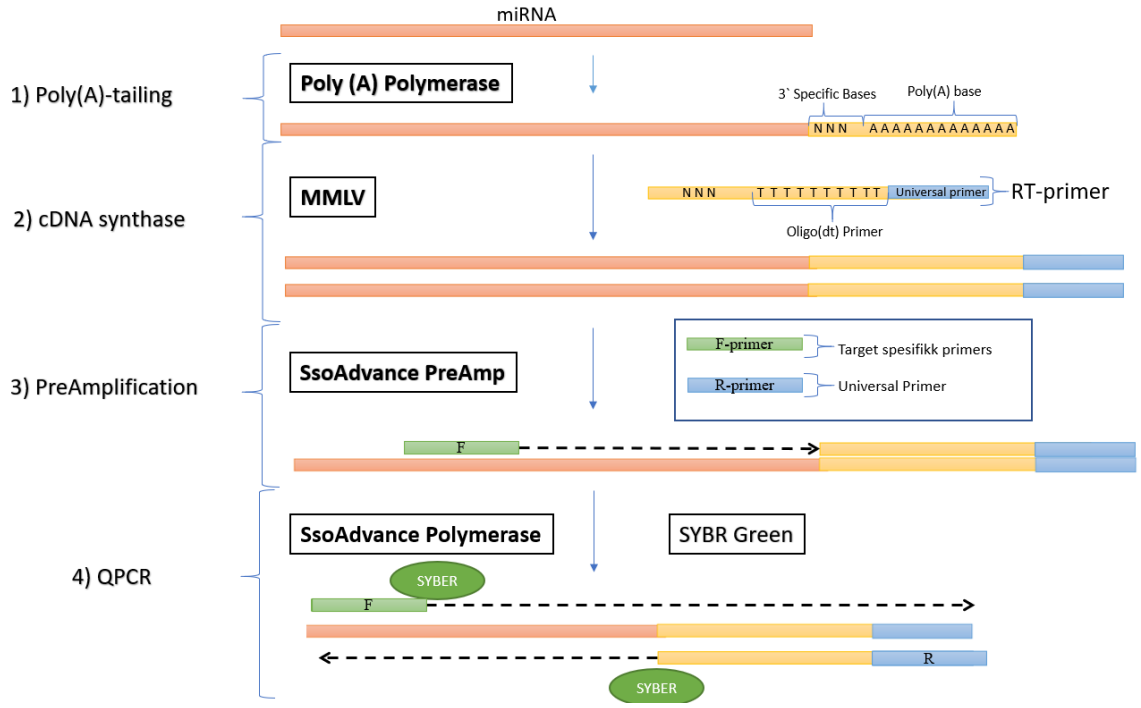

Figure 9: The complete workflow of miRNA expression shown in four steps. 1) Poly(A) tailing, a long adenine sequence, to improve primer hybridization. 2) Synthesis of cDNA by reverse transcriptase. 3) preamplification of primer segmented cDNA, primers used are from miRNA of interest (Table 6) (4) The miRNA expression analysis done on the PreAmplefied cDNA using SsoAdvance Polymerase coupled with Power SYBR green.

Because of the big sample size (n=1248) they would all be distributed across Thirteen Tear-A-way 96-well PCR plate (4Titude, Brooks Life Science) (96x13=1248) each being mixed with a Master mix coupled with the specific forward-primer, for miRNA of interest and distributed across four FameStar 386-well PCR plate (4ti-0385, Brooks Life Science) (Column four of the fourth plate)

Poly(A)-Tailing

Poly(A) tail is already present in mature mRNA making it an ideal primer target, the total RNA previously isolated also contains small RNA (miRNA) which does not have this tail. Using PAP coupled with ATP and buffer, containing co-factors for optimal enzymatic activity, a7 bp sequence of polyadenylates (Figure 9,1) was made at the 3` ends of small RNAs. This tail will be a capture sequence for oligo (dT) tagged with an RT-Primer (figure 9,2), suitable for reverse transcriptase.

The Master mix was prepared in a 15mL-falcone tube by adding PAP and components shown in table a (Poly(A) tailing) with pipette. The Master mix would further be mixed with reverse transcriptase components as shown in table a (cDNA).

Revers transcription

The isolated RNA would be revers transcribed to synthesize cDNA using Murine leukemia virus high performance reverse transcriptase (MMLV HP RT). mainly 3 types of primers could be used for inducing revers transcription: specific-, Oligo(dT)-, and random-primers. Since we include poly(A) tailing, the oligo(dT) primers would additionally be tagged with a RT-Primer. The RT-oligo(dT) primer is suitable for hybridization of both Poly(A) tail and MMLV HP RT. Also, to specify binding, a three base tag was added at the 3`of the molecule. This tag is specific for the miRNA of interest (Figure 9.2). Then 10µL diluted RT-pooled oligos and 10µL thawed RNA-sample was mixed in a new Tear-A-way 96-well PCR plate (4Titude, Brooks Life Science), then incubated at 65°C for 5min (Table 4, Template). The Master mix previously made was mixed with MMLV HP RT and components shown in table 4 (cDNA) The master mix was transferred to Reagens-reaservoir (Cat: 613-3194, VWR), where 20µL of the mix was pipetted to a Tear-A-way 96-well PCR plate (4Titude, Brooks Life Science) contenting previously prepared RNA-samples mixed with RT-oligo(dT) primers. The plate was sealed and placed at 24°C for 2min. cDNA synthesis was done by placing the samples in a thermal cycler with conditions shown in table 5.

Table 4: Components (µL) used for the coupled poly(A) tailing, cDNA synthesis and the Template of interest. Amplification would be done on the newly synthesized cDNA.

	Component	Volume (µL)
Poly (A) tailing	10x Poly(A) Polymerase Reaction Buffer	2
	ATP (10mM)	2
	Poly(A) Polymerase	2
	RiboLock RNase Inhibitor	1
cDNA	MMLV HP RT 10x Reaction Buffer	4
	dNTP mix (10mM)	4
	RNase-Free Water	3
	MMLV Reverse Transcriptase	2
Template	RNase-Free Water	-
	Isolated RNA	10
	RT Primer + RNase-free water	5+5
	Total Mix For cDNA Synthesis	40

Table 5: shows what conditions the thermal cycler used on the samples.

	Cycles	Step	Temp (°C)	Time (min)
Poly(A)-tailing cDNA Synthase		Synthesis	37	60
		Inactivation	95	5
	1	Hold	4	-

The product was aliquoted by transferring 20µL synthesized cDNA to a new Tear-A-way 96-well PCR plate (4Titude, Brooks Life Science) for downstream cDNA amplification. The cDNA concentration was measured using 2µL sample on the nanodrop dt-100. A Non transcription control was made containing 2µL synthesized cDNA pooled in one tube and stored.

Preamplification of specific candidate miRNAs using SsoAdvance PreAmp super kit.

Enrichment of synthesized cDNA by amplification was necessary because of the low quantity of RNA in plasma samples (> 10pg/µL). The SsoAdvanced PreAmp super mix kit was used to amplify the cDNA yield in our samples. The kit uses a fusion protein; a Taq-polymerase enzyme fused with the double-stranded binding-protein Sso7d. Resulting in a polymerase-complex with increased processivity, stability and reduced reaction time. The samples were placed in a thermal cycler, under condition shown I table 7. The cDNA, segmented by F- and R-Primers would be continuously amplified by the polymerase, enriching the concentration of the samples (Figure 9,3).

- **Pooled forward primer** was prepared by adding 10µL of each (n=17) forward primer (Table 6), diluted with 44.31mL RNase-free water in an 15mL-centrifuge tube, mixed by vertexing. 600µL was aliquoted, centrifuged, and stored in at -20°C.
- **Pooled revers primer** was made by adding 100µL Revers primer (Universal), diluted in 2,5mL RNase-free water in an 15mL-centrifuge tube, mixed by vertexing. 100µL was aliquoted, centrifuged, and stored in freezer at -20°C.
-

Table 6: Components used for Amplification of miRNA of interest using pooled primers, 17 forward primers and 1 universal revers prime.

	Component	Volume (µL)
Amplification	SsoAdvance PreAmp Super mix	25
	Primer -F/-R	4,5/0,5
	cDNA Template*	20
	Total Reaction for cDNA amplification	50

In an 15mL-centrifuge tube, 25µL SsoAdvanced PreAmp super mix, 4,5µL Forward primer and 0,5µL Revers primer was added as shown in Table 6. Then 25µL SsoAdvanced PreAmp super mix was transferred to the Tear-A-way 96-well PCR plate (4Titude, Brooks Life Science) containing 20µL of the previously aliquoted cDNA samples. Using a thermal cycler witch conditions shown in table 7, the cDNA would be PreAmplefied.

Tabell 7: table showing the conditions the thermal cycler was set to use.

Cycles	Step	Temp (°C)	Time (min)
1	Activation	95	3
20	Denaturing	95	0,25
	extension	58	4
1	Hold	4	-

Using the Nanodrop™ 1000 spectrometry (Fisher Scientific, Norway) 2µL preamplified cDNA-samples was used to quantify cDNA concentration. Then a pooled preamplified cDNA-samples was made by aliquoted 2µL of the samples to an Eppendorf tube to be checked for potential contaminations. The remaining preamplified plates was diluted with 50µL RNasefree-water, then the plate was sealed and stored at -20°C.

Quantitative Polymerase Chain reaction; qPCR

QPCR is a well-established method to explore expression of genes. There are several other methods to achieve the same goal, such as next generation sequencing or gene expression micro arrays. Although these methods are highly capable of giving adequate insight for the

purpose of this study, both methods rely on verification from qPCR, which is considered as the golden standard. In this study the relevant RNA is well known and simply relatively quantifying them is enough to identify potential biological markers. The qPCR is easily available and uses small amounts of sample, making it suitable for expression of candidate RNA in this study. Real-time qPCR gives real time observation of the exponential enrichment of sample. The rapid growth is caused from cyclic polymerization of sample nucleic acids. Each cycle is divided into three stages; denaturation, annealing and hybridization, each stage has an ideal condition/temperature to which during:

Denaturation the double stranded nucleic acids would separate making 2 complementary strands, usually the highest temperature possible without denaturing the polymerase. 95°C is commonly used coupled with a Taqman-polymerase.

Annealing is the most temperature specific step, and it is the step where the primers will hybridize to template. Tm is a value is where the equilibrium of primer-template complex is at 50%, Tm is calculated based on the primer's base composition. the annealing temperature (Ta) which is recommended to be 5°C lower than Tm should be the ideal conditions for annealing. If this temperature is to low an increase in nonspecific binding would accrue to high and no primers will bind.

extension phase requires a temperature that the polymerase has optimal biological activity. Usually this is around 70°C, and it's possible to couple annealing and extension in the same procedure such that after the first primer is hybridized the extension process can take place. To further ensure optimal polymerase condition enough amounts of the cofactor's magnesium chloride and magnesiumsulfat should be added.

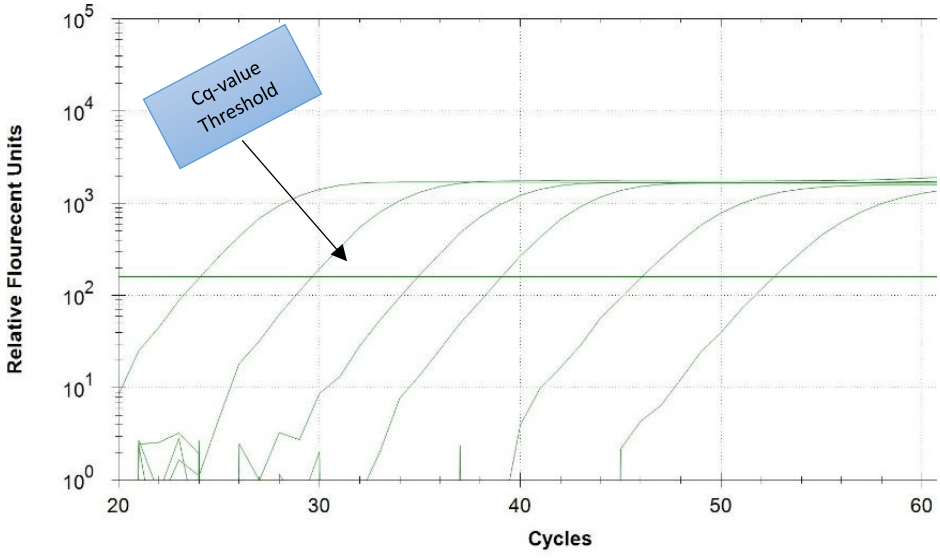

Figure 10: The reported Cq-value of a given sample, illustrates the threshold being placed above background noise. A samples relative fluorescent doubles with an efficiency ~2 for each cycle (x-axis). All samples have the same relative fluorescent increase; thus, the starting yield of RNA in a sample determines the number of cycles a sample need to cross the threshold.

The results after qPCR is reported as quantitative cycles (Cq) this number the numbers of cycle a sample needs to reach a fluorescent light (figure 10). A threshold at a desired fluorescent intensity (Figure 10) is placed to compare Cq-values between samples.

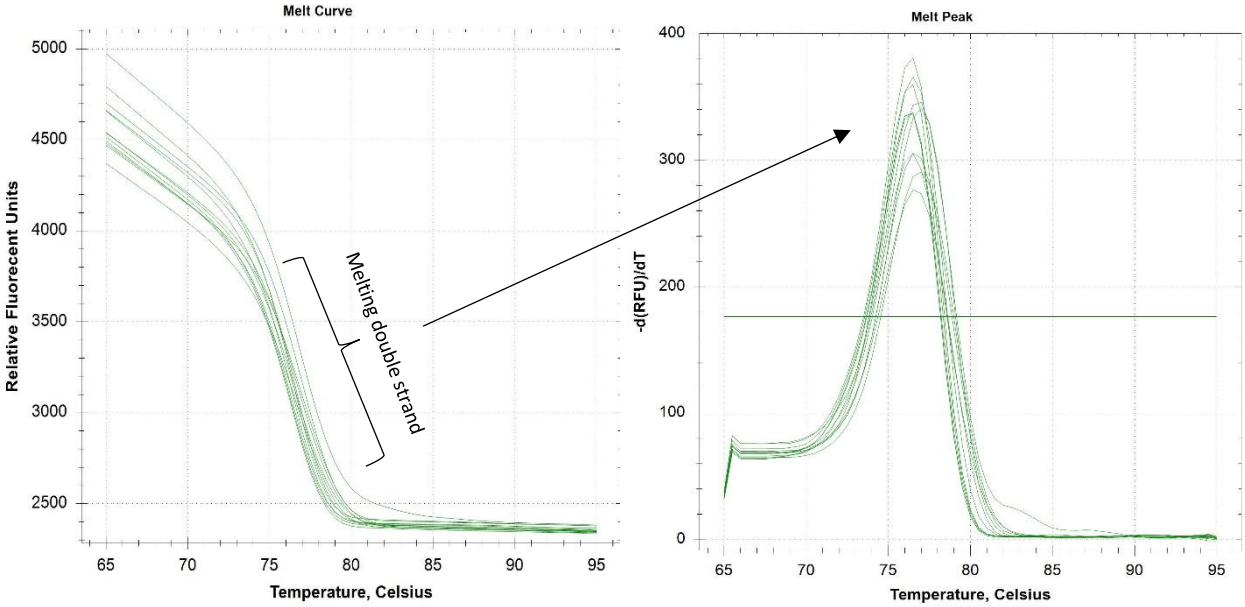

Figure 11: melt curve analysis report both melt curve A) and melt peak B). A) shows the rate at which SYBR green binds to double stands as relative fluorescent units (RUF), and how RFU change with a temperature increase. One can observe the degradation or what's referred to as melting of double strands, the fluorescent decreases as there are no double strand for SYBR Green to bind. B) the same report as in A) however data is presented as a derivative, thus, a district peak for when samples are melted is reported. Multiple different curves or peaks is evidence of unspecific binding or primer dimer formation.

The detection of each qPCR product requires a fluorophore, different fluorophores are available on the market. Probe specific fluorophore, which irreversibly releases fluorophore consecutively as the probe is degraded by polymerase. Or a nonspecific double stranded binding dye, which reversibly bind to dsDNA, and acts as a fluorophore when bound. The detected relative fluorescent is plotted as a graph against the number of cycles the sample has undergone. As shown in Figure 10 the growth of relative fluorescent. The probe-based

fluorophore is more specific, since it is reporting synthesis of new template. The dye would only bind dsDNA. Thus, the amount of fluorescent light is corresponding to amount of dsDNA. This concept decreases its specificity, because the increased possibility of false positive being detected from that primer dimers or nonspecific bindings, however SYBR green dye is cheaper (70).

In this study, SYBR green dye was used to investigate miRNA expression, because of the dye's specificity a melt-curve analysis should be done. A melt-curve analysis would gradually increase the temperature for each sample, while measuring the fluorescent light. As the temperature increases the dsDNA would form increasing fluorescent intensity, and at a temperature the dsDNA would be denatured, removing the fluorescent intensity shown Figure 11. These results heavy depends on what type of dsDNA strand that's formed, it would be considered nonspecific binding when the results shows multiple melt point peaks(70).

POWER SYBR green PCR Mastermix (Themo Fisher Scientic, Norway) was thawed at 4°C at least 3 hours before use. Separately, Forward Primer for relevant miRNA, and pooled revers primer was thawed on ice. 50µL preamplifier cDNA was transferred to a new Tear-A-Way 96-well PCR plate (4Titude, Brooks Life Science) and diluted in 195µL RNasefree-Water. The plates were sealed using Sealing Tape, clear polyester (Cat:236370, Thermo Scientific), marked "preAmp cDNA", stored at 4°C, and was used for subsequent miRNA expression.

Master mix was made in an 15mL-centrifugetube, mixing the components as shown in table 1. the master mix was transferred to Integra Reagens-reaservoir (Cat: 613-3194, VWR) and 163µL was distributed across the 7 first columns in a Tear-A-Way 96-well PCR plate (4Titude, Brooks Life Science), sealed using Sealing Tape, clear polyester (Cat:236370, Thermo Scientific), and place on ice.

Table 5: shows components used when making master mix, forward primer is specific for the miRNA that is wished to investigate.

	Component	Volume (µL)
Real-Time qPCR	Universal SYBR Green Mix	5
	F-Primer (specific, n=16)	0,5
	R-Primer (Universal)	0,5
	Reamplified cDNA*	4
	Total	10

Using the APS machine (Axygen, Norway), cooling blocks and Axygen robotic tips FX-50 (Cat: AXYGFX, VWR) 4µL master mixed was distributed to four FameStar 386-well PCR plate (4ti-0385, Brooks Life Science), then covered with aluminum seal tape (Cat: 232698, VWR) and stored at 4°C. The 13 Tear-A-Way 96-well PCR plate (4Titude, Brooks Life Science) marked "preAmp cDNA" was vortexed and centrifuged for 1 min in 4°C with 1500rpm, and 6µL "preAmp cDNA" was transferred the same four FameStar 386-well PCR plate (4ti-0385, Brooks Life Science) containing master mix.

The FameStar 386-well PCR plate (4ti-0385, Brooks Life Science) was sealed using Opti-Seal Optical disposable adhesive and placed on the real-time polymerase chain reaction machine (BioRad, Hercules, CA, USA). The plates "preAmp cDNA" was sealed using Sealing Tape, clear polyester (Cat:236370, Thermo Scientific) and stored at 4°C for future runs.

qPCR control

There are a few controls that should be included when running a PCR to confirm the integrity of the results. A Non transcription control was made control plate was made by making a dilution series from the 13-plate pooled cDNA Eppendorf tube. Four Eppendorf tubes was marked with "10x", "100x" "1000x" and "10 000x" and placed on ice. In the Eppendorf tube marked "10x" 20µL pooled cDNA was diluted with 180µL RNase-free water. A column was filled with 20µL from the previously diluted tube ("10X") and 180µL RNase-free water. Two replicas of 90µL from the dilution series was transferred and diluted with 90µL RNase-free water.

The second control was filled with 180µL RNase-free water, the plate was then sealed using Sealing Tape, clear polyester (Cat:236370, Thermo Scientific) and stored at 4°C. The control plate was carefully vortexed and centrifuged for 1 min in 4°C with 1500rpm. The FameStar

386-well PCR plate (4ti-0385, Brooks Life Science) was used to mix 4µL master mix with both the 6µL dilution series and 6µL RNase-free water from the control plate.

Relative gene expression

The efficiency of PCR should be estimated before transformation of miRNA expression, this is necessary when transforming Cq-values to relative quantity. In theory the efficiency of PCR is 100%, meaning that for each cycle, the PCR product would be doubled. Normally several conditions could compromise this efficiency, if the efficiency is just assumed the calculated quantity will fluctuate from true quantity(71).

The data was normalized based on three spike-in synthetic miRNA (table cel-miR). Using the normalization method(72), the function 2 and 4 is correspondingly used to transform Cq-value to a relative quantity, and normalize the values based on a normalization factor (function 2-3)

$$RQ = Efficiency(2)^{(Cq_{min} - Cq_{miRNA})} \quad (2)$$

$$NF = Efficiency(2)^{(Cq_{Geo,min} - Cq_{Geo\mu})} \quad (3)$$

$$Normalized\ RQ = \left(\frac{RQ}{NF}\right) \quad (4)$$

RQ is the relative quantity of our samples, Cq_{miRNA} is the miRNA expression, and the smallest value detected as Cq_{min}. NF is the normalization factor calculated using the geometric mean $Cq_{Geo\mu}$ of the spike-In and $Cq_{Geo,min}$.

Target genes/primer design.

In this project we investigated free circulating miRNA expression of 16 miRNAs, which has been reported to target at least four candidate ADHD genes (69)(table 6, ADHD targeted miRNA). The investigation was performed on archived plasma samples. The aim to investigate free circulation miRNA means that the plasma quality should not be compromised by cell leakage, specifically, the samples should not be hemolyzed. To assess the degree of hemolysis, an expression-based hemolysis score was made. Using two primers that targeted has-miR-451 and has-miR-23a-5p each known for being stably present in respectively, plasma and erythrocytes (14, 63) (table 6, control). To analyze the gene expression the normalized relative quantities was calculated for each measurement, normalization was based the expression of the added cel-miR (table 6, Synthetic miRNA)

Table 6: The primers used to target plasma miRNA in samples. Hemolysis controls primers used to calculate the ΔCq-score, shown in Function 2-3. Spike in, synthetic

	Primer	Targets
ADHD targeted miRNA	has-miR-335-5p	20
	has-miR-34a-5p	10
	has-miR-16-5p	7
	has-miR-125a-3p	5
	has-miR-21-5p	5
	has-miR-9-5p	5
	has-miR-19a-3p	4
	has-miR-204-5p	4
	has-miR-22-3p	4
	has-miR-616-5p	4
	has-miR-15a-5p	4
	has-miR-19b-3p	4
	has-miR-30a-5p	4
	has-miR-24-3p	4
	has-miR-155-5p	4
	has-miR-17-5p	4
Control	has-miR-451	Hemolysis
	has-miR-23a	Hemolysis
Synthetic miRNA	cel-miR-238	Spike-in
	cel-miR-54	Spike-in
	cel-miR-239	Spike-in

Statistical Analysis/Method

The statistics program JMP® Pro 15.0 on windows was used to report means standard deviation (SE) and create graphs. The statistical analyses ware done after the assumption for statistical tests were reported, the non-normal distributed variables was $\log_2$-transformed and checked for normality and equal variance using Shapiro Willks-test, and Levene`s-test. The robustness of the tests allows for some deviation in assumption (73). Still, the remaining non-normal variables ware inspected using the normal quantile plot to approve descent normality and find outliers Correlation between multiple variables ware done using Pearson pairwise correlation. Means of variables ware compared using the student`s t-tests. One-way Analysis of variance (ANOVA) was used to compare groups, given a significant result, the post hoc Tukey honestly significant different test was used to compare variables within a group. To determine significant predictors for a case a logistic regression was used, and predictor ware removed based of the Akaike`s information criterion (AIC) model. Results ware significant if the p-value ware greater then α-level (0.05).

Result

Comparisons of plasma quality control parameters

Preanalytical blood sample handling may affect plasma quality and consequently on RNA quality and stability. Therefore, the plasma quality was assessed with several methods in order to determine the impact of preanalytical sample handling on plasma quality. A comparison of the different plasma quality control parameters is shown in Table 7

Table 7: Plasma quality control parameters are presented as cord paternal and maternal plasma samples. Plasma quality control parameters separated into cord, paternal and maternal plasma samples.

	Method	Cord			Paternal			Maternal			All samples		
		Mean	SE	N	Mean	SE	N	Mean	SE	N	Mean	SE	N
UV-vis spectrometer (Nanodrop)	A414	0,666	0,025	408	0,296	0,011	406	0,211	0,007	412	0,391	0,011	1226
	A541	0,112	0,005	408	0,113	0,005	406	0,079	0,004	412	0,101	0,003	1226
	A576	0,096	0,004	408	0,085	0,004	406	0,058	0,002	412	0,079	0,002	1226
	LIHS-SCORE	0,398	0,018	408	0,059	0,005	404	0,049	0,004	412	0,168	0,008	1224
qPCR-Based assay	$\Delta Cq_{(23a-451)}$	3,402	0,084	413	2,746	0,073	409	2,880	0,056	413	3,010	0,042	1235
Particle count (Casy counter)	Microparticles	11138	926	413	18922	994	411	11105	677	413	13713	516	1237
	Platelets	2100	118	413	5504	426	411	3296	262	413	3630	175	1237
	Total particle count	17171	1016	403	25974	1619	398	19281	1109	399	20792	743	1200

Note. Standard error (SE) and N = number of analyzed sample size. Plasma quality control parameters separated into cord, paternal and maternal plasma samples.

Plasma hemolysis assessment

In this project, we are interested to identify potential candidate circulating miRNA markers of ADHD in plasma samples, any miRNA contamination from exogenous sources may obscure result integrity. Therefore, quantifying plasma hemolysis is essential as it's an indication of contamination from blood components (e.g. red blood cells). Assessment of the impact of preanalytical sample handling on plasma quality is very important step and will increase the confidence of the downstream analysis results. Therefore, three different methods were used to quantify hemolysis in the plasma samples:

i) Visual score: plasma samples were graded into four hemolysis levels (0, 1, 2, 3) based on visual assessment of the samples Figure 12 B). The distribution of the 1248 plasma samples divided into hemolysis grade levels are presented in Figure 12 A). Compared with paternal

and maternal plasma samples, most of the cord plasma samples were graded as hemolysis level 2 or 3, and only 6.5% of samples were graded as hemolysis level 1. Further, none of the plasma samples were graded as hemolysis level 0. On the other hand, paternal and maternal plasma samples had correspondingly 90.5% and 79.4% of samples in hemolysis level 1.

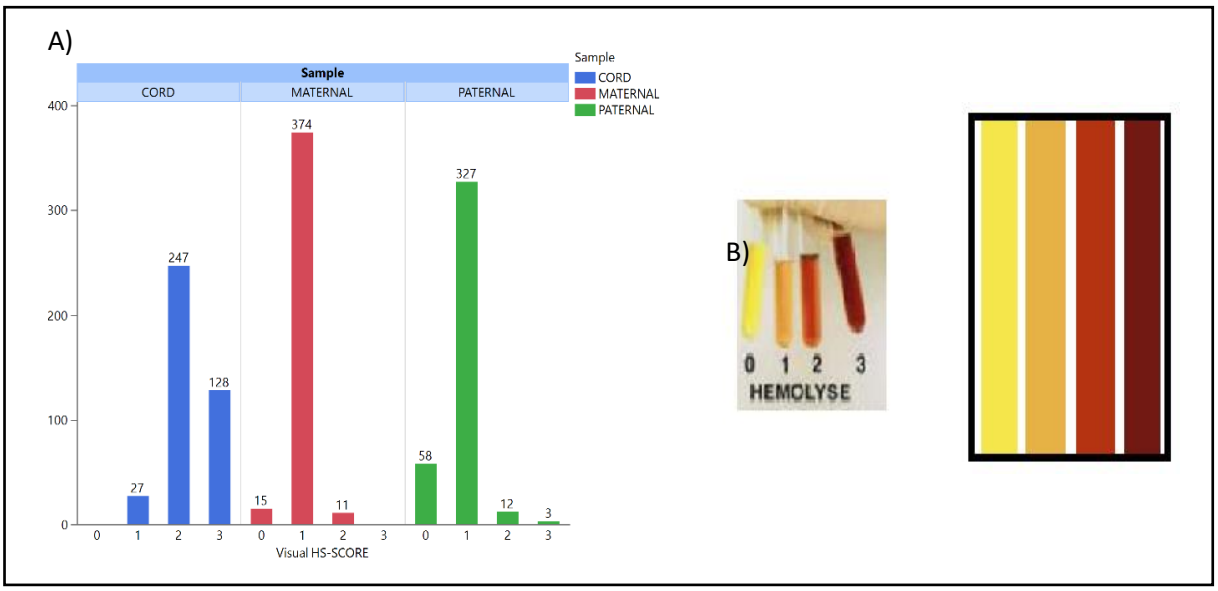

Figure 12: A) The results of grading 1248 plasma samples based on haemolysis level. Most of cord (blue) samples are graded 2-3 while the adult samples (red, green) ware graded 1. B) Plasma with different haemolysis levels, used as a reference for grading plasma samples. Increasing discolouration of plasma indicates higher degree of haemolysis.

ii) Spectrometer UV-vis analysis of plasma samples by Nanodrop instrument: this method measures plasma discoloration intensity, by quantifying the absorbance of the samples across a UV-vis spectrum (Figure 13). The presence of absorbances peak at 414 (Figure 13 A), 541 (Figure 13 B) and 575 nm (Figure 13 C) indicates hemolysis. These peaks are a measure for the presence of hemoglobin in the plasma samples and it is the source of red discoloration (Figure 5). First, the mean intensity at 414nm from all samples was 0.39±0.38, but as shown in (Figure 12 A) this mean is heavily skewed by cord plasma samples. The mean intensity at 541 nm and 575 nm was correspondingly 0.10±0.09 and 0.08±0.076, respectively. There were significant differences between cord and adult samples in at 414, 541 and 576 nm. However, pairwise comparison revealed cord and paternal plasma samples had no significant difference in either at 541 nm or at 576 nm ($p>0.05$). Noteworthy, the 414 nm results with a hemolysis threshold of 0.2 as shown in Figure 13 is not in line with the visual hemolysis grade level, which seems to be excluding multiple samples that have a hemolysis grade level 1.

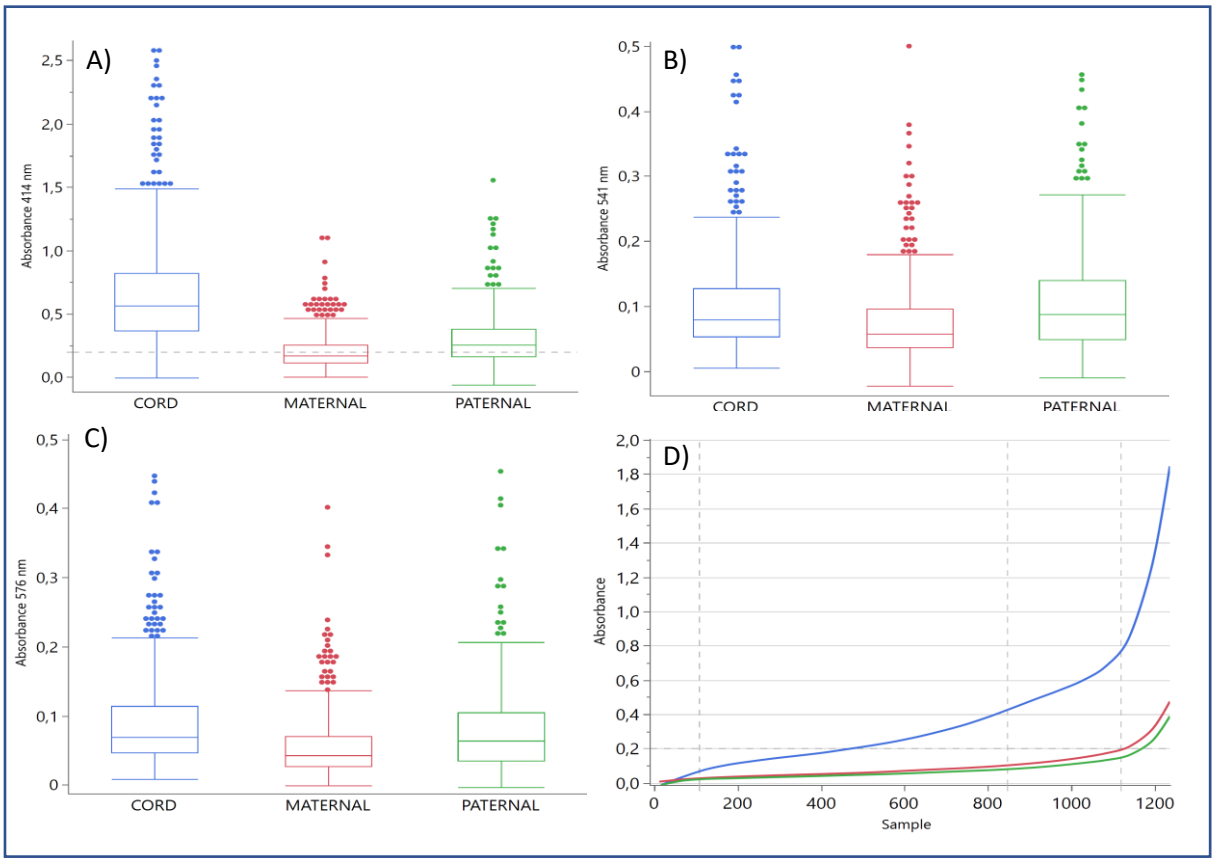

Figure 13: Shows the boxplot of hemolysis parameters. Distribution of absorbance measurements of A414 (A), A541(B) and A575(C), Cord samples showing a different A414 measurement compared to paternal and maternal samples, threshold is set at an A414 measurement of 0.2. (D) showing samples result ordered ascendingly for hemolysis parameters. Vertical lines are the grade intervals and horizontal is the hemolysis threshold.

The LIHS-score is calculated based on lipemia-independent Hemolysis score (LIH-score). The LIHS-score was defined by the sample absorbance at 414 nm and 385 nm. The LIHS-score distribution is shown in figure 14. The average LIHS-score for cord, maternal, and paternal samples were 0.40±0.02, 0.05±0.011 and 0.06±0.01, respectively. No statistically significantly differences between the maternal and paternal samples was observed, while cord samples were significantly higher ($P<0.001$) then maternal, and paternal samples (Figure 14 A). The LIHS-score seems to follow the same pattern as the visual grading of samples (Figure

14 B). However, in this case the LIHS-score threshold is set to 0.057 (very strict threshold) which seems to be excluding multiple samples that have a hemolysis grade level 1.

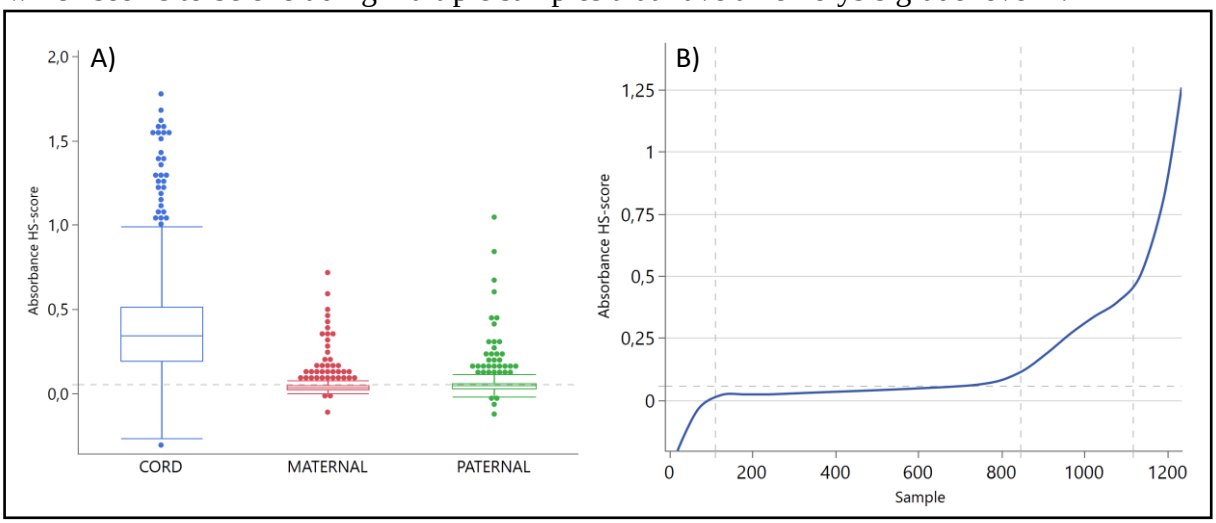

Figure 14: A) Boxplot of absorbance LIHS-score across the triad, show that the mean LIHS from cord in substantially higher than that observed in adults. B) The absorbance LIHS-Score calculated by A414 and A385. Threshold set to be at 0.057.

iii) qPCR-based method: the method is based on measuring the difference between two miRNAs, miR-23a and miR-451 shown in Table 6. The expression level of these two miRNAs is compared and the difference between the is a measure for hemolysis expressed as ΔCq-score.

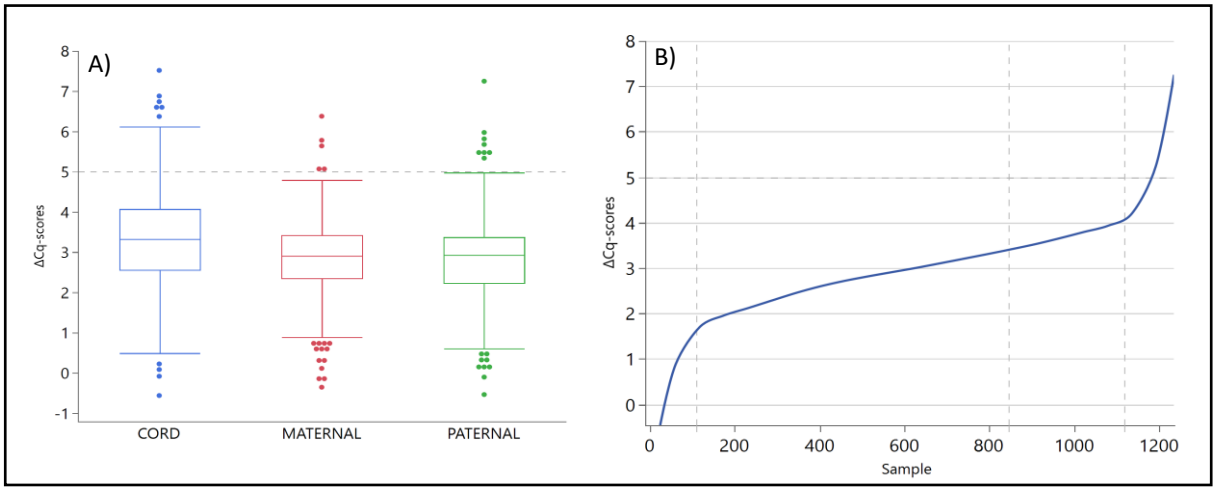

Figure 15: The Distribution of the delta value from expression analysis of hsa-miR-451 and –23a, shown as a boxplot with cord paternal and maternal samples. Horizontal doted at the ΔCq-score of 5 as the threshold

For the ΔCq-score with a threshold of 5, most of the plasma samples were considered as not hemolyzed. Further, the average ΔCq-score of all plasma samples was 3.01±1.5. The average ΔCq-scores for cord, paternal and maternal plasma samples were 3.40±1.70, 2.75±1.5 and 2.88±1.14, respectively (Figure 15 A). The ΔCq-score correspond well with the visual score results (Figure 15 B). However, this ΔCq-score allows some samples graded as level 3 to be

included. Cord samples have a significantly higher ΔCq-score than paternal and maternal samples ($p<0.001$), while there was no significant difference between the paternal and the maternal samples ($p=0.19$).

Particle counts

The number of particles in the plasma samples were analyzed using CASY cell counter (Roche, Norway) with a particle size threshold of less than 5µm. Platelets have a diameter of 2-5µm, while microparticles have a diameter less than 1.5 µm. The average total particle count for plasma samples was 20843±25872 counts, while for platelets and microparticles were 3642±6167 counts and 13731±18125 counts, respectively (shown in Figure A-C).

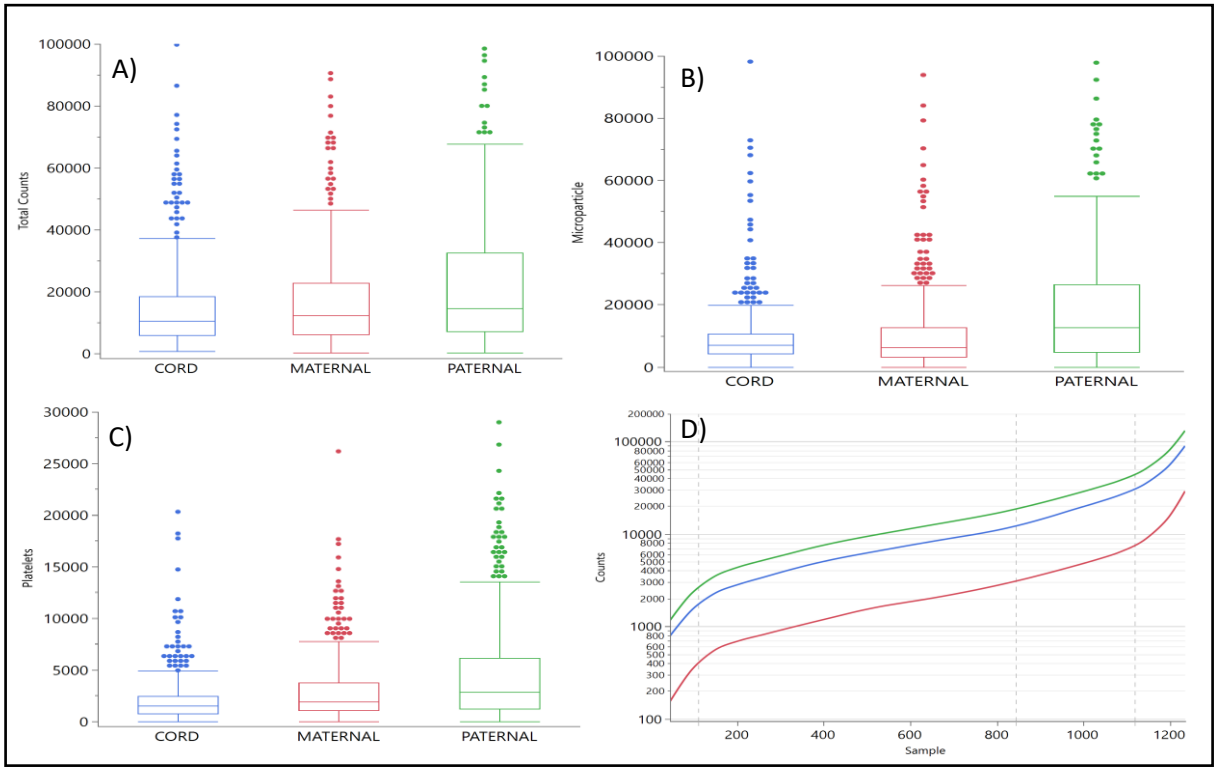

Figure 16: A boxplot showing distribution of particle counts as the size range of microparticles (A), Platelets (B), Total (C). Platelet counts is clearly lower than MP count, additionally there were significant difference between cord, maternal and paternal counts. There was no significant difference in microparticle count of cord and maternal sample ($p=0.938$). D) Particle counts shown for total, microparticle and platelets ascendingly ordered samples. Microparticles and platelets count is crossing the grade level 2 at correspondingly 15 000 and 3000 counts.

The average particle counts within microparticle size range were in average above 10 000 counts/µL, while particles within platelet size range had an average counts less than 6000 counts. observed between the three groups ($p<0.001$). Pairwise comparison showed that there was no significant difference in microparticle counts between cord and maternal samples ($p=0.938$). There was significant difference between microparticle and platelet count ($p<0.001$). When plasma samples grouped into cord, maternal and paternal, a statistically

significant differences in counts was observed. Figure 16 D shows that there was a 10-fold difference between microparticle, and platelets counts in samples with grade level 1, indicating good quality samples. The results from particle counting reported 31 samples with higher counts then 100.000, all of which resides in grade 3.

Plasma QC summarized

Finally, the different plasma quality control parameters were compared (Figure 17). As expected, the quality control parameters measured with the Nanodrop correlated well with each other, i.e., A414, A541 and A576 had a strong correlation between them (Figure 1). Further, there was a weak correlation between A541 or A576 and the LIHS-score (R^2<0.43). However, the LIHS-score correlated well with the A414 (R^2=0.81). This is important, because the LIHS-score was calculated based on the measurements of A414 and A385. The particle count quality control parameters measured with the Casy instrument correlated well with each other (Figure 17). There was a strong correlation between microparticle and platelet counts (R^2=0.81), while their correlation with total counts was weaker (R^2<0.43). An interesting observation was that the A541 and A576 measurements had a weak but noticeable correlation with particle count parameters such as microparticle and platelet counts (R_2 = (0.30 – 0.42)). When it comes to the qPCR-based plasma quality control parameter, the ΔCq (miR-23a-miR-451)-score had very weak correlation with the other plasma quality control parameter (Figure 17).

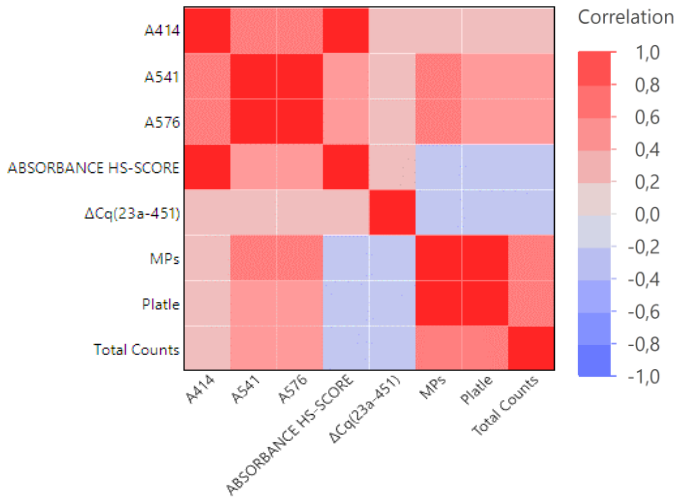

Figure 17: The correlation matrix based on how the different plasma QC parameters correlate to each other. Correlation reported as a scale from 1 to -1.

Plasma RNA Quantification

It is necessary to quantify plasma RNA amount before downstream miRNA expression analysis. The obtained RNA amount from plasma samples are usually very low and they are under the limit of detection for most of the common quantification methods, thus a qPCR-

based RNA amount quantification kit “Low Abundance RNA Quantification Kit” was used. The kit is based on both relative quantifications, using a specially synthesized primers that amplifies a wide variety of RNAs. The standard curve shown in 18 was used to calculate the mean RNA concentration of 16 plasma samples. The regression line created using standards included in Low Abundance RNA Quantification Kit. Cycles plotted as a function of concentration shown as log values.

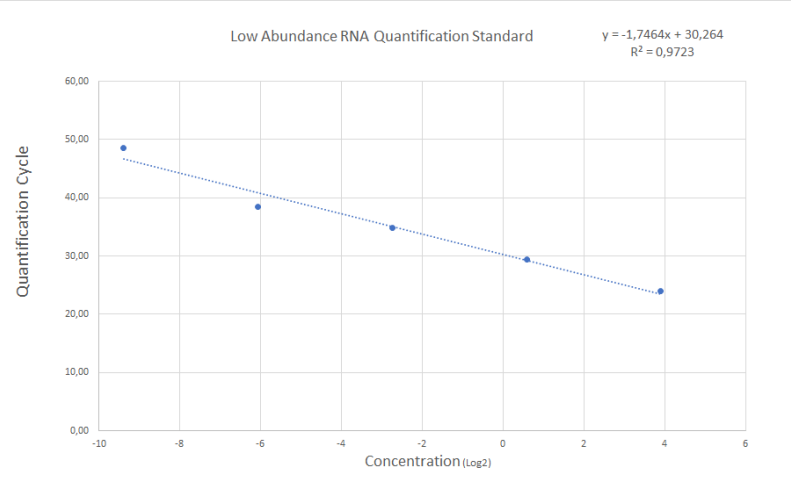

Figure 18: The regression line created using synthetic RNA standards included in Low Abundance RNA Quantification Kit. Cycles plotted as a function of concentration shown

The RNA expression level of the standard curve shown in Figure 18 gave a slope of -1.764 with a $R^2 = 0.972$ and a concentration ratio of 1/4.9 between standard curve and the plasma samples. Based on the standard curve the plasma sample RNA concentration can be estimated. The RNA isolated from the plasma samples had an average RNA concentration of 1.40 ± 0.53 pg/µL, ranging from 0.01–10 pg/µL. From the plasma samples an average of 1.0 – 50 pg RNA was obtained. This finding confirms the need for RNA concentration quantification methods that can measure RNA concentration down to fg/µL range.

miRNA expression analysis.

The miRNA expression profile of 16 selected miRNAs was performed by qPCR assay from the 1248 plasma samples consisting of ADHD cases (n = 208 case-parent triads) and matched controls (n = 208 control-parent triads). First, investigating miRNA expressed differently between cord, maternal and paternal samples would probably give some indication about a potential preanalytical sample handling effects on the miRNA expression profiles. This is true for cord blood plasma samples where the preanalytical sample handling were no optimal. Many cord plasma samples had poor quality as shown in Figure 19. The average $\log_2$ -transformed miRNA expression levels ($\log_2$-NRQ values) for cord, paternal and maternal samples were 0.83±0.12, -0.89±0.12 -0.79±0.12, respectively (Figure 19).

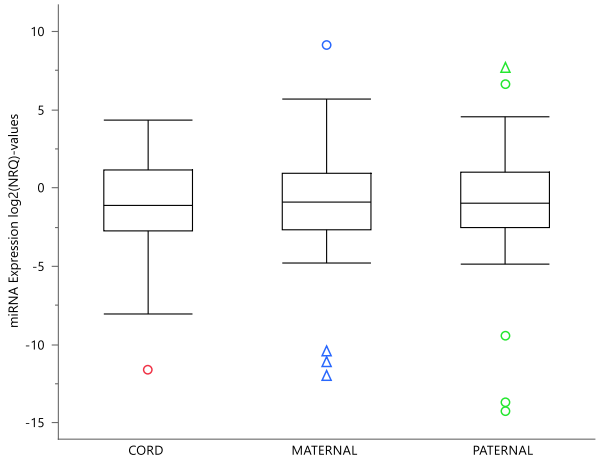

Figure 19: The average log_2NRQ-values of all miRNAs (n=16 miRNAs) for the cord, maternal and paternal samples are shown in the boxplot. The boxplots show median, outliers, skewness and degree of dispersion of the data. Theirs a slight difference between the mean expression of cord samples then observed in either paternal or maternal samples, suggesting different miRNA expression profile in cord samples.

In Figure 19, the relative miRNA expression level difference (log2-fold change) between cord-maternal, cord-paternal and maternal-paternal are shown. For the comparison groups, the relative miRNA expression levels showed some differences (Figure 19); however, the expression level changes were well within ± twofold, except for the expression levels of miR-17-5p, miR-155-5p, and miR-204-5p for the cord-maternal comparison, and the expression levels of miR-17-5p and miR-19a-3p for the maternal-paternal comparison (Figure 19).

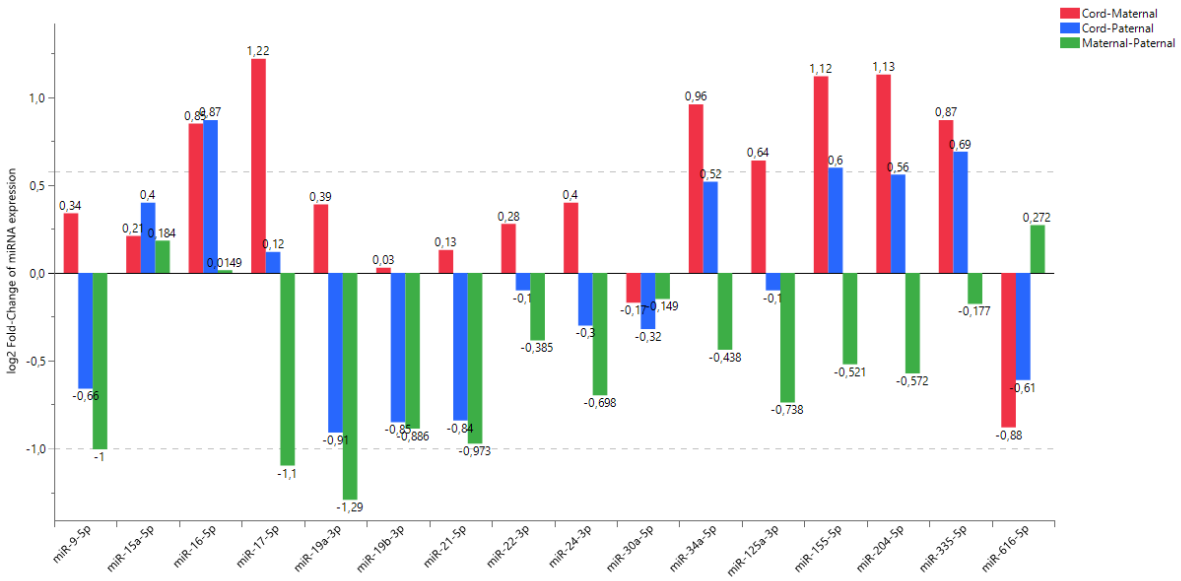

Figure 20: The log_2-transformed fold change of NRQ-transformed miRNA expression, shown between cord-paternal (blue), cord-maternal (red) and maternal-paternal (green), and for each miRNA of interest. The horizontal stippled lines illustrate the ± 2-fold.

A statistical comparison of the miRNA expression levels of the cord, maternal and paternal samples is presented in Table 8. There were no statistically significantly differently expressed miRNAs between the cord, maternal and paternal samples (Table 8). Further, when the miRNA expression level for maternal and paternal samples were combined as one group "Adults" and compared with cord plasma samples, two miRNAs (miR-155-5p (p=0.017) and miR-15a-5p (p=0.036)) were suggested as statistically significantly differently expressed between the groups (Table 8).

Table 8: Comparison of the miRNA expression levels of cord, maternal and paternal samples

	CORD	MATERNAL	PATERNAL	ANOVA	Cord-Adults	
miRNA	Mean ± SE	Mean ± SE	Mean ± SE		p-value	Log_2 FC
miR-616-5p	1,68 ± 0,13	3,08 ± 1,37	2,55 ± 0,58	0,902	0,973	-0,75
miR-335-5p	10,60 ± 5,06	5,81 ± 0,81	6,57 ± 1,91	0,426	0,523	0,78
miR-204-5p	9,81 ± 4,02	4,49 ± 0,68	6,68 ± 2,04	0,425	0,224	0,81
miR-155-5p*	3,01 ± 0,98	1,39 ± 0,21	1,99 ± 0,49	0,067	0,017*	0,83
miR-125a-3p	1,36 ± 0,50	0,87 ± 0,20	1,46 ± 0,59	0,718	0,561	0,22
miR-34a-5p	6,41 ± 2,97	3,30 ± 0,54	4,47 ± 1,15	0,671	0,521	0,72
miR-30a-5p	0,36 ± 0,05	0,40 ± 0,08	0,44 ± 0,14	0,925	0,960	-0,25
miR-24-3p	0,27 ± 0,06	0,20 ± 0,03	0,33 ± 0,11	0,696	0,473	0,01
miR-22-3p	1,69 ± 0,24	1,39 ± 0,18	1,82 ± 0,50	0,307	0,392	0,08
miR-21-5p	0,35 ± 0,07	0,32 ± 0,04	0,63 ± 0,24	0,811	0,720	-0,44
miR-19b-3p	2,07 ± 0,33	2,02 ± 0,33	3,74 ± 1,50	0,775	0,513	-0,48
miR-19a-3p	1,94 ± 0,54	1,49 ± 0,23	3,64 ± 1,82	0,801	0,521	-0,40
miR-17-5p	2,31 ± 0,95	1,00 ± 0,12	2,13 ± 0,95	0,569	0,474	0,57
miR-15a-5p*	8,18 ± 1,63	7,06 ± 1,38	6,21 ± 1,02	0,660	0,036*	0,30
miR-16-5p	0,60 ± 0,24	0,33 ± 0,05	0,33 ± 0,05	0,095	0,777	0,86
miR-9-5p	3,41 ± 0,72	2,69 ± 0,42	5,40 ± 2,60	0,842	0,796	-0,25

Note. log_2 -fold-change (FC), and p-value is reported for ANOVA test done between the cord and Adult, a group that's the average of maternal and paternal expression. Significance at α-level (p<0.05).

Comparison between ADHD cases and controls

The miRNA expression level difference between ADHD cases and matched controls of cord plasma samples was performed and presented in Table 9 and Figure 21. No statistically significantly differentially expressed miRNA between ADHD-cases and matched controls was observed (Table 9).

Table 9: The expression level of miRNA shown for ADHD cord samples and control, also shown is an comparison analysis using students t-test

	$ADHD_{n=150}$			$CTL_{n=164}$			ADHD-CTL	
miRNA	mean	SE	n	mean	SE	n	p-value	Log_2 FC
616-5p	1,62	± 0,16	150	1,73	± 0,21	164	0,622	-0,10
335-5p	5,04	± 0,98	147	15,99	± 9,92	164	0,231	-1,66
204-5p	5,43	± 1,30	149	14,11	± 7,86	164	0,236	-1,38
155-5p	2,73	± 1,04	150	3,29	± 1,67	164	0,969	-0,27
125a-3p*	0,85	± 0,16	150	1,86	± 0,97	164	0,055	-1,13
34a-5p	3,21	± 0,63	150	9,56	± 5,86	163	0,637	-1,57
30a-5p	0,32	± 0,05	150	0,39	± 0,10	164	0,560	-0,28
24-3p	0,24	± 0,05	149	0,30	± 0,12	164	0,665	-0,33
22-3p	1,88	± 0,44	150	1,50	± 0,21	164	0,536	0,33
21-5p	0,33	± 0,08	150	0,37	± 0,11	164	0,604	-0,14
19b-3p	2,15	± 0,44	150	2,00	± 0,48	162	0,505	0,10
19a-3p	2,46	± 1,03	148	1,43	± 0,34	163	0,954	0,78
17-5p*	1,34	± 0,34	150	3,27	± 1,85	164	0,096	-1,28
15a-5p	6,75	± 1,03	150	9,59	± 3,08	164	0,139	-0,51
16-5p	0,38	± 0,09	150	0,82	± 0,47	163	0,565	-1,09
9-5p	3,55	± 0,96	150	3,27	± 1,08	164	0,775	0,12

Note. Mean and standard error (SE) for ADHD and CTL of cord samples. Difference in miRNA expression between cord ADHD and CTL shown with p-value, and the log_2- fold change. Significance at α-level (p=0.05)

However, two miRNAs; miR-17-5p (p=0.096, FC=-1.28) and miR-125a-3p (p=0.055, FC=-1.38) were borderline significant. For ADHD-cases, the expression level (log_2-NRQ-values) for most of the analyzed miRNAs were lower than the control samples (Figure 21).

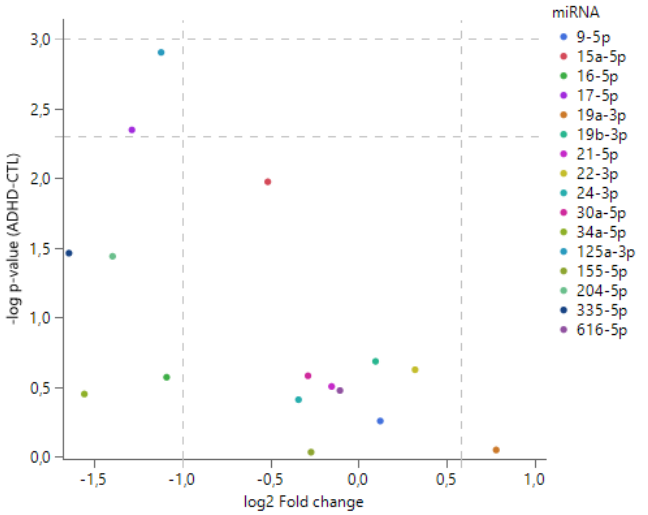

Figure 21: A volcano plot showing -log-transformed p-values from Table 9 plotted against the log_2 fold-change between ADHD-cases and control samples. Vertical dotted lines are the fold change range (-1<FC<1) and horizontal line are α-levels of p<0.05. These two miRNAs; miR-17-5p (p=0,055) and miR-125a-3p (p=0,095) has high fold change between ADHD-cases and controls.

Comparison of parent-ADHD cases and parent-controls.

Since we found miRNA in the cord ADHD-case group that ware borderline significantly different from control group. Further, evaluating whether these miRNAs are exclusively differently expressed in cord samples compared to maternal and paternal samples should be done. Paternal and maternal ADHD cases are defined by the offspring's (cord) diagnosis. Firstly, the fold change miRNA from paternal samples varied to a higher degree then observed from maternal samples. Secondly, significantly differently expressed miRNA between ADHD-cases and controls for both paternal and maternal samples (Table 10), showed no significantly differently expressed miRNAs between them. There is an overall higher p-value for the cord comparison of miRNA expression (Table 9, Figure 21) between ADHD-cases and controls then seen between paternal and maternal samples.

Table 10: Mean miRNA expression of ADHD and CTL reported for paternal and maternal samples.

	ADHD		CTL		Paternal n=185		Maternal n=204	
	Paternal	Maternal	Paternal	Maternal				
miRNA	Mean ± SE	Mean ± SE	Mean ± SE	Mean ± SE	p-value	Log_2 FC	p-value	Log_2 FC
616-5p	3,02 ± 1,05	1,70 ± 0,21	2,08 ± 0,51	4,47 ± 2,75	0,30	0,54	0,78	-1,39
335-5p	7,63 ± 3,58	5,81 ± 1,23	5,53 ± 1,42	5,81 ± 1,06	0,65	0,46	0,79	0,00
204-5p	8,08 ± 3,90	3,97 ± 0,57	5,28 ± 1,25	5,02 ± 1,24	0,74	0,61	0,48	-0,34
155-5p	1,82 ± 0,47	1,14 ± 0,19	2,17 ± 0,87	1,64 ± 0,38	0,06	-0,25	0,71	-0,52
125a-3p	1,00 ± 0,47	0,61 ± 0,09	1,90 ± 1,07	1,14 ± 0,39	0,74	-0,92	0,38	-0,91
34a-5p	5,57 ± 2,17	2,97 ± 0,48	3,37 ± 0,77	3,64 ± 0,98	0,63	0,72	0,91	-0,30
30a-5p	0,52 ± 0,26	0,34 ± 0,10	0,36 ± 0,09	0,46 ± 0,11	0,86	0,53	0,52	-0,42
24-3p	0,42 ± 0,21	0,19 ± 0,04	0,24 ± 0,08	0,22 ± 0,03	0,41	0,83	0,46	-0,20
22-3p	2,15 ± 0,93	1,21 ± 0,17	1,49 ± 0,36	1,58 ± 0,32	0,29	0,53	0,67	-0,39
21-5p	0,80 ± 0,45	0,30 ± 0,06	0,45 ± 0,19	0,34 ± 0,05	0,94	0,82	0,5	-0,17
19b-3p	5,15 ± 2,94	2,00 ± 0,57	2,34 ± 0,69	2,05 ± 0,31	0,91	1,14	0,56	-0,03
19a-3p	5,37 ± 3,53	1,40 ± 0,40	1,87 ± 0,70	1,58 ± 0,24	0,32	1,52	0,45	-0,18
17-5p	1,38 ± 0,57	0,94 ± 0,15	2,87 ± 1,80	1,05 ± 0,18	0,77	-1,06	0,98	-0,17
15a-5p	7,01 ± 1,90	5,91 ± 0,95	5,43 ± 0,75	8,22 ± 2,60	0,69	0,37	0,79	-0,48
16-5p	0,31 ± 0,07	0,34 ± 0,06	0,35 ± 0,08	0,33 ± 0,09	0,43	-0,16	0,83	0,07
9-5p	8,22 ± 5,17	2,52 ± 0,70	2,59 ± 0,60	2,86 ± 0,45	0,70	1,66	0,38	-0,18

Note. log_2 -fold-change (FC), and p-value is reported for ANOVA test done between the cord and Adult, a group that's the average of maternal and paternal expression. Significance at α-level ($p<0.05$).

Since we have good information about how the family sample from ADHD-case group relate to their corresponding control group, we can be certain that the observation from cord samples are unique compared to paternal and maternal samples (Table 10) as the p-values of miRNAs is overall standing out as lower than that of paternal and maternal.

Logistic regression of ADHD-cases and controls based on cord samples.

Logistic regression analysis is a robust method to evaluate the degree a single miRNA could predict ADHD in cord samples (n=302). Since there were only two miRNAs that could be

considered borderline significantly differently expressed between ADHD-cases and controls in the previous analysis, it is expected to not find any robust miRNA predictor of ADHD in the logistic regression analysis, but it will tell how much it relies on each miRNA based on the estimated coefficient. Thus, preforming logistic regression on the miRNAs and evaluating the coefficient applied to a miRNA will indicate the degree a miRNA can predict ADHD in the context of all miRNAs (n=16).

Table 11: Logistic regression coefficient for each miRNA. The "Total" row is the logistic regression using all miRNA (n=16), "significant" row is the logistic regression done after removal of miRNAs to improve AIC-value (ΔAIC=19).

	miRNA	Coefficient	SE	P-value	95% CI	
					Lower	Upper
total p=0.63 AIC=440	miR-616-5p	0,11	0,09	0,22	-0,06	0,28
	miR-335-5p	-0,10	0,14	0,44	-0,38	0,17
	miR-204-5p	-0,01	0,12	0,93	-0,26	0,24
	miR-155-5p	-0,05	0,07	0,46	-0,18	0,08
	miR-125a-3p	-0,28	0,18	0,12	-0,66	0,05
	miR-34a-5p	0,04	0,08	0,62	-0,11	0,23
	miR-30a-5p	0,08	0,09	0,37	-0,10	0,26
	miR-24-3p	0,44	0,26	0,09	-0,07	0,96
	miR-22-3p	0,02	0,19	0,91	-0,32	0,47
	miR-21-5p	-0,16	0,15	0,28	-0,49	0,11
	miR-19b-3p	0,06	0,14	0,64	-0,20	0,34
	miR-19a-3p	0,02	0,14	0,87	-0,25	0,30
	miR-17-5p	0,13	0,23	0,58	-0,33	0,58
	miR-15a-5p	-0,08	0,16	0,61	-0,39	0,23
	miR-16-5p	0,06	0,06	0,36	-0,06	0,18
	miR-9-5p	-0,25	0,22	0,26	-0,68	0,18
	miR-21-5p	-0,11	0,11	0,31	-0,34	0,10
	miR-9-5p	-0,14	0,16	0,38	-0,46	0,17
Significant p<0.05 AIC=421	*miR-616-5p**	*0,12*	*0,06*	*0,05*	*0,00*	*0,24*
	miR-125a-3p*	-0,27	0,10	0,01*	-0,47	-0,09
	miR-24-3p*	0,45	0,20	0,03*	0,06	0,86

Note. Mean and standard error (SE) for ADHD and CTL of cord samples. Difference in miRNA expression between cord ADHD and CTL shown with p-value, and the log_2- fold change. Significance at α-level (p=0.05)

Logistic regression preformed on all miRNAs found no significantly contributing miRNAs (p=0.63), the AIC was used as a selection criterion to stepwise to remove miRNA which does not contribute to the model's precision. Removal of these miRNAs; miR-155-5p miR204-5p, miR-19a-3p, miR-19b-3p, miR-15a-5p, miR-34a-5p, miR-17-5p, miR-335-5p and miR-30a-

5p, and miR-16-5p improved the model (AIC=421) (Table 11). After step-wise eliminating miRNAs, three miRNAs; miR-125a-3p (p=0.005) with an estimate of -0.27±0.10, miR-24-3p (p=0.0216) with an estimate of 0.45±0.20 and miR-616-5p (p=0.045) with an estimate of 0.12±0.06 (Table 11), were identified as predictor for ADHD and these miRNAs can be used to distinguish between ADHD-cases and controls (Table 11). Interesting finding was miR-125a-3p, this miRNA was also found to be statistically significant in the previous (T-test) analysis.

Logistic regression prediction of ADHD based on maternal or paternal sample.

To further investigate miRNAs miR-125a-3p, miR-24-3p and miR-616-5p identified as significant in the ADHD-cases predictive model, logistic regression was used for paternal (n=366) and maternal (n=389) miRNAs (Table 12). Logistic regression on all miRNA (n=16) did not yield any significantly contributing miRNAs for paternal (p=0.199, AIC=523) or maternal (p=0.864, AIC=565) samples.

Table 12: Logistic regression coefficient for each miRNA of interest reported with the standard error

	miRNA	Coefficient	SE	p-value	95% CI	
					Lower	Upper
Total p=0,199 AIC=523	miR-616-5p	0,078	0,080	0,33	-0,07	0,24
	miR-335-5p	-0,148	0,158	0,35	-0,46	0,16
	miR-204-5p	-0,207	0,215	0,33	-0,63	0,21
	miR-155-5p	0,112	0,056	0,05	0,01	0,23
	miR-125a-3p	-0,105	0,177	0,55	-0,46	0,23
	miR-34a-5p	0,110	0,175	0,53	-0,23	0,46
	miR-30a-5p	-0,033	0,087	0,70	-0,21	0,14
	miR-24-3p	0,201	0,230	0,38	-0,25	0,66
	miR-22-3p	0,204	0,205	0,32	-0,15	0,65
	miR-21-5p	-0,052	0,093	0,57	-0,26	0,12
	miR-19b-3p	-0,180	0,151	0,23	-0,50	0,10
	miR-19a-3p	0,093	0,122	0,44	-0,13	0,36
	miR-17-5p	0,037	0,237	0,88	-0,44	0,50
	miR-15a-5p	0,005	0,124	0,97	-0,24	0,25
	miR-16-5p	-0,133	0,072	0,06	-0,28	0,01
	miR-9-5p	0,008	0,207	0,97	-0,40	0,42
Significant p=0,041 AIC=510	miR-155-5p*	0,104	0,052	0,04	-0,04	0,23
	miR-125a-3p*	-0,214	0,106	0,04	0,01	0,22
	miR-16-5p*	-0,118	0,056	0,03	-1,13	-0,11

Note. (SE) and p-value estimating the significance of a miRNA in the model. The "Total" row is the logistic regression using all miRNA), "significant" row is the logistic regression with improve AIC-value.

Step-wise removing miRNAs from the paternal model; miR204-5p, miR-21-3p, miR-19b-3p, miR-15a-5p, miR-335-5p, miR-17-5p, miR-335-5p and miR-616-5p, and miR-24-5p, based on the AIC model improved the model significantly (p=0.041, ΔAIC=13). The miRNAs with

significantly contributing in the model are miR-155-5p (p=0.04) with coefficient of 0.104±0.052, miR-125a-3p (p=0.04) with the coefficient -0.214±0.106 and miR-16-5p (p=0.03) with the coefficient of -0.118±0.056.

Although the logistic regression using all miRNAs (n=16) showed miR-125a-3p (p=0.05) and miR-17-5p (p=0.03) as significant predictors in this model (Table 13)). Further removal of miRNA based on the AIC model, improved the AIC-value (ΔAIC=16), however, this did not improve the significance of other miRNAs then miR-125-3p (p=0.032) with the coefficient of -0,347± 0,162 and miR-17-5p (p=0.028) with a coefficient of 0.4524±0,206

Table 13: Logistic regression coefficient for each miRNA of interest reported with p-value estimating the significance of a miRNA in the regression model.

					95% CI	
	miRNA	Coefficient	SE	p-value	Lower	Upper
Total p=0,864 AIC=565	miR-616-5p	-0,007	0,068	0,92	-0,14	0,13
	miR-335-5p*	0,009	0,135	0,95	-0,26	0,27
	miR-204-5p	-0,109	0,131	0,41	-0,41	0,12
	miR-155-5p	0,014	0,041	0,73	-0,07	0,09
	miR-125a-3p*	-0,354	0,178	0,05	-0,72	-0,03
	miR-34a-5p	-0,017	0,108	0,88	-0,23	0,20
	miR-30a-5p	-0,004	0,076	0,96	-0,15	0,15
	miR-24-3p	0,115	0,197	0,56	-0,27	0,51
	miR-22-3p*	-0,246	0,246	0,32	-0,74	0,23
	miR-21-5p	0,020	0,103	0,85	-0,19	0,22
	miR-19b-3p*	0,100	0,130	0,44	-0,15	0,36
	miR-19a-3p	-0,024	0,070	0,73	-0,17	0,11
	miR-17-5p*	0,522	0,244	0,03	0,06	1,02
	miR-15a-5p*	0,179	0,120	0,14	-0,05	0,42
	miR-16-5p	0,003	0,055	0,96	-0,11	0,11
	miR-9-5p	-0,221	0,186	0,23	-0,59	0,14

Note. (SE) and p-value estimating the significance of a miRNA in the model. The "Total" row is the logistic regression using all miRNA (n=16), "significant" row is the logistic regression done after removal of miRNAs to improve AIC-value.

Discussion

It has been shown that multiple disorders are related to miRNAs(74), and that miRNAs could be used as a diagnostic marker for these disorders (75). Over the recent years the literature investigating miRNAs and their role in ADHD have increased (6, 31, 76, 77). There is also extensive evidence on miRNA integrity and its association with quality of plasma samples (78), more specifically, how pre-analytic handling (65) and freeze thaw cycles (66) can

introduce exogenous components to free-flowing miRNA in plasma. This study investigated whether miRNAs targeting ADHD candidate genes were differentially expressed between cord blood plasma samples of ADHD cases and controls, as well as performing a screening of multiple quality-control parameters.

We investigated samples gathered by the Norwegian mother father and child cohort study. Firstly, the screening showed that the samples were not ideal for miRNA expression, due to the observed trend of high hemolysis measurements of cord samples. However, there was no significant difference in these measures between ADHD cases and controls ($p>0.05$), and any difference in miRNA expression levels could therefore still be relevant. Secondly, two miRNAs were reported as downregulated and considered borderline significant between cord ADHD cases and controls; miR-125a-3p and miR-17-5p. Further investigation of these miRNAs could be of great importance in the search for biomarkers of ADHD.

Plasma quality.

The reason multiple parameters were measured was to ensure rich amounts of plasma quality information was available, as there are uncertainties around what parameters are significant when determining the plasma quality. There was no correlation between hemolysis measurements and particle counts, additionally there was no correlation between the ΔCq-score and any of the measurements. There seems to be clear evidence that discoloration is not something that can reliably be measured with spectrometry or is related to particle counts.

Hemolysis

The visual inspection and grading of plasma samples highlighted that most cord samples had a grade between level 2-3, while both maternal and paternal samples were largely grade level 1. The same observation of cord samples was observed by spectrophotometry measures of A414 with a threshold for hemolysis of $A414<0.2$ (65). Most cord samples resided above this threshold and were significantly higher than both paternal and maternal samples ($p>0.05$). Interestingly, there were cord samples with a visual grade level 3, that showed A414 measurements below the threshold, suggesting discoloration is not always detected by this method.

MoBa`s visual assessment of the cord plasma samples reported 21 and 42% of samples resided within grade level 0 and 1 respectively, and only 26 and 10% resided respectively in grade level 2 and 3. It has been proposed that the pre-analytic handling of cord samples stored in biobanks for the MoBa study was improper, as the plasma was not separated from whole

blood at extraction date, which was done for maternal and paternal samples. The cord plasma samples are probably discolored because of this difference in analytic handling(13).

Measurements A541 and A576 interestingly reported no significant difference between cord and paternal samples ($p<0.05$), as cord samples with grades 2-3 have a similar mean as paternal samples with grade 1. This indicates that measurements of A541 and A576 are independent of discoloration, or it could be that the deoxyheamoglobin that is measured at A541 and A576 is oxidized over time.

Applying the LIHS-score proposed by Appierto, et al. (68) did reduce the number of hemolyzed cord samples, with a threshold of 0,057. There was no significant difference between maternal and paternal samples($p<0.05$). The paternal and maternal samples showed no difference between LIHS-score and A414 nm, this is probably since a larger A414 nm measurements is needed for lipemia-factor be implemented.

Although the spectrometric methods showed that the mean cord measurements were above the threshold, ΔCq-score does not show the same results. The difference between the cord grades and the paternal and maternal grades are also clear in the ΔCq-score. Since the ΔCq-score is a direct comparison between steadily present miRNAs in erythrocytes and plasma, it is regarded as a robust and reliable measure of hemolysis, (14, 65).

Particle count

The particle counts of microparticles and platelets ware promising. Mitchell (66) have suggested that non-contaminated platelet plasma would contain approximately $191x10^3$ counts, however, as shown in our results the average total particle count was $20,8x10^3$, and particle counts done in the platelet range ware lower than that. This could be because the study utilized standard complete blood count (CBC) and counted fluorescently labeled platelets using flowcytometry. Our counting instrument is based on the Coulter principle. A comparison between the methods (79) showed that flowcytometry is preferred as it is reporting platelets specifically. Still, the Coulter principle was the commercially available predecessor. Since the measuring methods don't explain the difference in platelets, as one would not expect lower counts in an instrument with lower specificity. It might indicate that the preanalytical handling of the samples managed to remove vast amounts of platelets.

Further the main source of particles counted ware microparticles, and the results showed a 10-fold increase in counts between microparticle and platelets. It has been suggested Mitchell,

Gray (66) that either the pre-analytic handling is not optimal for reducing microparticles, or that there are platelet derived microparticles introduced by freeze-thaw cycles (66).

The particle count results from cord samples did not seem to be affected by their visual grade. On the contrary, there was no significant difference in microparticle counts between cord and maternal samples($p>0.05$). Paternal samples showed a larger count of particles and microparticles than cord and maternal samples. This could be due to an interplay of sample extraction and handling. These findings suggest that there could be a possible skewing of miRNA expression level in paternal samples, relative to cord and maternal, due to higher counts of platelets and microparticles.

Expression of miRNA targeting ADHD candidate genes

The average relevant miRNA expression was lower for cord samples then paternal and maternal samples. This could report that there are miRNAs that is differently expressed in cord samples. However, it is also possible that this difference is caused by the different visual grade of cord samples, compared to maternal and paternal samples.

Addressing the main aim of this study, that is, investigating potential differently expressed miRNA between ADHD cases and controls from cord blood plasma samples. There was no miRNA that was significantly differentially expressed, however, miR-17-5p and miR-125a-3p, stood out as borderline significantly downregulated between the ADHD cases and controls.

A logistic regression analysis where the prediction model for ADHD was made based on the miRNAs (n=16), showed miR-17-5p and miR-125a-3p as well as miR-616-5p ware relevant for predicting ADHD based on cord samples. We found that the same logistic regresion analysis preformed on paternal and maternal samples showed miR-125a-3p as a relevant predictor, there were additional predictive miRNAs for paternal and maternal samples respectively; miR-155-5p miR-16-5p and miR-335-5p miR-19b-3p miR-17-5p miR-15a-5p.

These miRNAs target potential candidate ADHD genes that have been found to be present in multiple ADHD databases, as reported by Dypås et al. (69). Specifically, miR-125a-3p targets the five mRNAs GIT1 GRIN2A MTHFR EMP2 and NT5C2. miR-125a-3p has also been reported to have properties that alters morphology of synapses and plasticity (80), as well as cell proliferation and apoptosis (81). miR-17-5p was reported (69) to have four targets that are potential candidate ADHD genes; TRIM32 CLOCK ATXN1 and SLC6A4. miR17-5p is

commonly reported as miR-17-92 cluster, consisting of multiple miRNAs, some of which were included in our study; miR-19a-3p and miR-19b-3p. Overexpression of the miR-17-92 cluster has been shown to improve plasticity, and though the exact function is not clear it is associated with axonal outgrowth (82).

Dypås et al. (69) further reported that the normal gene expression of miR-125a-3p is stable across multiple life stages. They also found the miR-17-5p cluster to be overexpressed in infancy, but more stably expressed in subsequent life stages. MiR-125a-3p being stably expressed throughout normal development could explain why it is a significant variable in predictive models of ADHD for paternal and maternal samples. Our observations reported miR-17-5p as downregulated between ADHD and control, and there was no evidence of clustering of miR-19a-3p and miR-19b-3p. This might indicate that miR-17-5p in ADHD patients is not clustered with miR-19a-3p and miR-19b-3p, since it is downregulated. however, they reported miRNA expression in brain tissue which could be the reason these differences are present. additionally, miR-125-3p was found by (77) to be downregulated, although not significant. Even though their study isolated miRNAs from whole blood, which makes it hard to compare with our finding, it strengthens our results of miR-125-3p being borderline significant.

miR-125a-3p and miR-17-5p are also miRNAs that is reported in many other neurodevelopmental disorders. Unfortunately, there is poor overlap in the academic literature between these disorders. Additionally, miR-125a-3p and miR-17-5p have been reported to be promising biomarkers and predictors for multiple neurodevelopmental disorders as well as markers used to for cancer prognosis (83-85). .

Conclusion

In conclusion, the main goal of this thesis was to evaluate the quality of plasma samples isolated from cord, mother and father, and whether these plasma samples are of high quality to be used to identify predictive miRNAs. Overall, the plasma samples from the mothers and fathers' samples had a good quality; however, there was some issues with the cord plasma samples. The plasma quality of these samples was not optimal. Cord plasma samples were processed at NIPH, and there was a time lag between cord blood collection and the time when plasma was isolated from them. It is not certain whether these results have been skewed by hemolysis contamination.

The expression levels of 16 miRNAs regulating ADHD candidate genes were evaluated in order to identify differentially expressed miRNA between ADHD cases and matched controls. Two miRNAs, miR-125a-3p and miR-17-5p were identified as potential ADHD predictive markers distinguishing between ADHD cases from matched controls. These two miRNAs have a well-established role as biomarkers for multiple cancer types and involved in neuropsychological disorders closely related to ADHD.

It is not certain whether any of the remaining miRNAs would be significantly differentially expressed if the cord plasma samples had optimal quality. Also, worth noting, that the selection of miRNAs is tissue derived, and therefore, it is not necessarily expected that tissue specific miRNAs are observable as freely circulating miRNAs.

Reference

1. Jin P, Alisch RS, Warren ST. RNA and microRNAs in fragile X mental retardation. Nature Cell Biology. 2004;6(11):1048-53.
2. Camkurt MA, Karababa F, Erdal ME, Bayazıt H, Kandemir SB, Ay ME, et al. Investigation of Dysregulation of Several MicroRNAs in Peripheral Blood of Schizophrenia Patients. Clinical Psychopharmacology and Neuroscience. 2016;14(3):256-60.
3. Perkins DO, Jeffries CD, Jarskog LF, Thomson JM, Woods K, Newman MA, et al. microRNA expression in the prefrontal cortex of individuals with schizophrenia and schizoaffective disorder. Genome Biology. 2007;8(2):R27.
4. Sarachana T, Zhou R, Chen G, Manji HK, Hu VW. Investigation of post-transcriptional gene regulatory networks associated with autism spectrum disorders by microRNA expression profiling of lymphoblastoid cell lines. Genome Medicine. 2010;2(4):23.
5. Lukiw WJ, Zhao Y, Cui JG. An NF-κB-sensitive Micro RNA-146a-mediated Inflammatory Circuit in Alzheimer Disease and in Stressed Human Brain Cells. Journal of Biological Chemistry. 2008;283(46):31315-22.
6. Maes O, Chertkow H, Wang E, Schipper H. MicroRNA: Implications for Alzheimer Disease and other Human CNS Disorders. Current Genomics. 2009;10(3):154-68.
7. Kloosterman WP, Plasterk RHA. The Diverse Functions of MicroRNAs in Animal Development and Disease. Developmental Cell. 2006;11(4):441-50.
8. Chen X, Ba Y, Ma L, Cai X, Yin Y, Wang K, et al. Characterization of microRNAs in serum: a novel class of biomarkers for diagnosis of cancer and other diseases. Cell Research. 2008;18(10):997-1006.
9. Huang W. MicroRNAs: Biomarkers, Diagnostics, and Therapeutics. Springer New York; 2017. p. 57-67.
10. Lee YS, Dutta A. MicroRNAs in Cancer. Annual Review of Pathology: Mechanisms of Disease. 2009;4(1):199-227.
11. Wang TJ. Assessing the Role of Circulating, Genetic, and Imaging Biomarkers in Cardiovascular Risk Prediction. Circulation. 2011;123(5):551-65.
12. Magnus P, Irgens LM, Haug K, Nystad W, Skjærven R, Stoltenberg C. Cohort profile: The Norwegian Mother and Child Cohort Study (MoBa). International Journal of Epidemiology. 2006;35(5):1146-50.
13. Rønningen KS, Paltiel L, Meltzer HM, Nordhagen R, Lie KK, Hovengen R, et al. The biobank of the Norwegian mother and child cohort Study: A resource for the next 100 years. European Journal of Epidemiology. 2006;21(8):619-25.
14. Blondal T, Jensby Nielsen S, Baker A, Andreasen D, Mouritzen P, Wrang Teilum M, et al. Assessing sample and miRNA profile quality in serum and plasma or other biofluids. Methods. 2013;59(1):S1-S6.
15. Faraone SV, Asherson P, Banaschewski T, Biederman J, Buitelaar JK, Ramos-Quiroga JA, et al. Attention-deficit/hyperactivity disorder. Nature Reviews Disease Primers. 2015;1(1):15020.
16. Gizer IR, Ficks C, Waldman ID. Candidate gene studies of ADHD: a meta-analytic review. Human Genetics. 2009;126(1):51-90.
17. Polanczyk G, De Lima MS, Horta BL, Biederman J, Rohde LA. The Worldwide Prevalence of ADHD: A Systematic Review and Metaregression Analysis. American Journal of Psychiatry. 2007;164(6):942-8.
18. Dalsgaard S, Mortensen PB, Frydenberg M, Thomsen PH. ADHD, stimulant treatment in childhood and subsequent substance abuse in adulthood — A naturalistic long-term follow-up study. Addictive Behaviors. 2014;39(1):325-8.
19. Lichtenstein P, Halldner L, Zetterqvist J, Sjölander A, Serlachius E, Fazel S, et al. Medication for Attention Deficit–Hyperactivity Disorder and Criminality. New England Journal of Medicine. 2012;367(21):2006-14.

20. Dalsgaard S, Østergaard SD, Leckman JF, Mortensen PB, Pedersen MG. Mortality in children, adolescents, and adults with attention deficit hyperactivity disorder: a nationwide cohort study. The Lancet. 2015;385(9983):2190-6.
21. Young JL, Goodman DW. Adult Attention-Deficit/Hyperactivity Disorder Diagnosis, Management, and Treatment in the DSM-5 Era. The Primary Care Companion For CNS Disorders. 2016.
22. Anixt JS, Vaughn AJ, Powe NR, Lipkin PH. Adolescent Perceptions of Outgrowing Childhood Attention-Deficit Hyperactivity Disorder: Relationship to Symptoms and Quality of Life. J Dev Behav Pediatr. 2016;37(3):196-204.
23. Katzman MA, Bilkey TS, Chokka PR, Fallu A, Klassen LJ. Adult ADHD and comorbid disorders: clinical implications of a dimensional approach. BMC Psychiatry. 2017;17(1).
24. Jacob C, Gross-Lesch S, Jans T, Geissler J, Reif A, Dempfle A, et al. Internalizing and externalizing behavior in adult ADHD. ADHD Attention Deficit and Hyperactivity Disorders. 2014;6(2):101-10.
25. Kessler RC, Adler L, Barkley R, Biederman J, Conners CK, Demler O, et al. The Prevalence and Correlates of Adult ADHD in the United States: Results From the National Comorbidity Survey Replication. American Journal of Psychiatry. 2006;163(4):716-23.
26. Regier DA. Dimensional approaches to psychiatric classification: refining the research agenda for DSM-V: an introduction. International Journal of Methods in Psychiatric Research. 2007;16(S1):S1-S5.
27. Faraone SV, Perlis RH, Doyle AE, Smoller JW, Goralnick JJ, Holmgren MA, et al. Molecular Genetics of Attention-Deficit/Hyperactivity Disorder. Biological Psychiatry. 2005;57(11):1313-23.
28. Faraone SV, Larsson H. Genetics of attention deficit hyperactivity disorder. Molecular Psychiatry. 2019;24(4):562-75.
29. Chen Q, Brikell I, Lichtenstein P, Serlachius E, Kuja-Halkola R, Sandin S, et al. Familial aggregation of attention-deficit/hyperactivity disorder. Journal of Child Psychology and Psychiatry. 2017;58(3):231-9.
30. Manolio TA, Collins FS, Cox NJ, Goldstein DB, Hindorff LA, Hunter DJ, et al. Finding the missing heritability of complex diseases. Nature. 2009;461(7265):747-53.
31. Walton E, Pingault JB, Cecil CAM, Gaunt TR, Relton CL, Mill J, et al. Epigenetic profiling of ADHD symptoms trajectories: a prospective, methylome-wide study. Molecular Psychiatry. 2017;22(2):250-6.
32. Arnsten AFT, Li B-M. Neurobiology of Executive Functions: Catecholamine Influences on Prefrontal Cortical Functions. Biological Psychiatry. 2005;57(11):1377-84.
33. Pliszka SR, McCracken JT, Maas JW. Catecholamines in attention-deficit hyperactivity disorder: current perspectives. J Am Acad Child Adolesc Psychiatry. 1996;35(3):264-72.
34. Gainetdinov RR. Role of Serotonin in the Paradoxical Calming Effect of Psychostimulants on Hyperactivity. Science. 1999;283(5400):397-401.
35. Berridge CW, Devilbiss DM. Psychostimulants as Cognitive Enhancers: The Prefrontal Cortex, Catecholamines, and Attention-Deficit/Hyperactivity Disorder. Biological Psychiatry. 2011;69(12):e101-e11.
36. Biederman J, Monuteaux MC, Spencer T, Wilens TE, Faraone SV. Do stimulants protect against psychiatric disorders in youth with ADHD? A 10-year follow-up study. Pediatrics. 2009;124(1):71-8.
37. Thau L, Reddy V, Singh P. Anatomy, Central Nervous System. StatPearls. Treasure Island (FL): StatPearls Publishing

38. Hampel L, Lau T. Neurobiological Principles: Neurotransmitters. Springer International Publishing; 2020. p. 1-21.
39. Gail T, Jeffery RW. Neurobiology of ADHD. Neuropharmacology. 2009;57(7):579-89.

40. Arnsten AFT. Stimulants: Therapeutic Actions in ADHD. Neuropsychopharmacology. 2006;31(11):2376-83.
41. Caye A, Swanson JM, Coghill D, Rohde LA. Treatment strategies for ADHD: an evidence-based guide to select optimal treatment. Molecular Psychiatry. 2019;24(3):390-408.
42. Rosalind CL, Rhonda LF, Victor A. The C. elegans heterochronic gene lin-4 encodes small RNAs with antisense complementarity to lin-14. Cell. 1993;75(5):843-54.
43. Reinhart BJ, Slack FJ, Basson M, Pasquinelli AE, Bettinger JC, Rougvie AE, et al. The 21-nucleotide let-7 RNA regulates developmental timing in Caenorhabditis elegans. Nature. 2000;403(6772):901-6.
44. Pasquinelli AE, Reinhart BJ, Slack F, Martindale MQ, Kuroda MI, Maller B, et al. Conservation of the sequence and temporal expression of let-7 heterochronic regulatory RNA. Nature. 2000;408(6808):86-9.
45. Fire A, Xu S, Montgomery MK, Kostas SA, Driver SE, Mello CC. Potent and specific genetic interference by double-stranded RNA in Caenorhabditis elegans. Nature. 1998;391(6669):806-11.
46. Kim Y-K, Kim VN. Processing of intronic microRNAs. The EMBO Journal. 2007;26(3):775-83.
47. Friedman RC, Farh KKH, Burge CB, Bartel DP. Most mammalian mRNAs are conserved targets of microRNAs. Genome Research. 2008;19(1):92-105.
48. Iftikhar H, Carney GE. Evidence and potential in vivo functions for biofluid miRNAs: From expression profiling to functional testing. BioEssays. 2016;38(4):367-78.
49. Fromm B, Billipp T, Peck LE, Johansen M, Tarver JE, King BL, et al. A Uniform System for the Annotation of Vertebrate microRNA Genes and the Evolution of the Human microRNAome. Annual Review of Genetics. 2015;49(1):213-42.
50. Alles J, Fehlmann T, Fischer U, Backes C, Galata V, Minet M, et al. An estimate of the total number of true human miRNAs. Nucleic Acids Research. 2019;47(7):3353-64.
51. Carthew RW, Sontheimer EJ. Origins and Mechanisms of miRNAs and siRNAs. Cell. 2009;136(4):642-55.
52. O'Brien J, Hayder H, Zayed Y, Peng C. Overview of MicroRNA Biogenesis, Mechanisms of Actions, and Circulation. Frontiers in Endocrinology. 2018;9.
53. Alarcón CR, Lee H, Goodarzi H, Halberg N, Tavazoie SF. N6-methyladenosine marks primary microRNAs for processing. Nature. 2015;519(7544):482-5.
54. Denli AM, Tops BBJ, Plasterk RHA, Ketting RF, Hannon GJ. Processing of primary microRNAs by the Microprocessor complex. Nature. 2004;432(7014):231-5.
55. Ha M, Kim VN. Regulation of microRNA biogenesis. Nature Reviews Molecular Cell Biology. 2014;15(8):509-24.
56. Okada C, Yamashita E, Lee SJ, Shibata S, Katahira J, Nakagawa A, et al. A High-Resolution Structure of the Pre-microRNA Nuclear Export Machinery. Science. 2009;326(5957):1275-9.
57. Tomoko K, Yukihide T. Making RISC. Trends in Biochemical Sciences. 2010;35(7):368-76.
58. Dharap A, Pokrzywa C, Murali S, Pandi G, Vemuganti R. MicroRNA miR-324-3p Induces Promoter-Mediated Expression of RelA Gene. PLoS ONE. 2013;8(11):e79467.
59. Krützfeldt J, Rajewsky N, Braich R, Rajeev KG, Tuschl T, Manoharan M, et al. Silencing of microRNAs in vivo with 'antagomirs'. Nature. 2005;438(7068):685-9.
60. Ameres SL, Horwich MD, Hung JH, Xu J, Ghildiyal M, Weng Z, et al. Target RNA-Directed Trimming and Tailing of Small Silencing RNAs. Science. 2010;328(5985):1534-9.
61. Jonas S, Izaurralde E. Towards a molecular understanding of microRNA-mediated gene silencing. Nature Reviews Genetics. 2015;16(7):421-33.
62. Mitchell PS, Parkin RK, Kroh EM, Fritz BR, Wyman SK, Pogosova-Agadjanyan EL, et al. Circulating microRNAs as stable blood-based markers for cancer detection. Proceedings of the National Academy of Sciences. 2008;105(30):10513-8.
63. Turchinovich A, Weiz L, Langheinz A, Burwinkel B. Characterization of extracellular circulating microRNA. Nucleic Acids Research. 2011;39(16):7223-33.
64. Gallo A, Tandon M, Alevizos I, Illei GG. The Majority of MicroRNAs Detectable in Serum and Saliva Is Concentrated in Exosomes. PLOS ONE. 2012;7(3):e30679.

65. Kirschner MB, Kao SC, Edelman JJ, Armstrong NJ, Vallely MP, Van Zandwijk N, et al. Haemolysis during Sample Preparation Alters microRNA Content of Plasma. PLoS ONE. 2011;6(9):e24145.
66. Mitchell AJ, Gray WD, Hayek SS, Ko Y-A, Thomas S, Rooney K, et al. Platelets confound the measurement of extracellular miRNA in archived plasma. Scientific Reports. 2016;6(1):32651.
67. Shet A. Characterizing blood microparticles: Technical aspects and challenges. Vascular Health and Risk Management. 2008;Volume 4:769-74.
68. Appierto V, Callari M, Cavadini E, Morelli D, Daidone MG, Tiberio P. A lipemia-independent NanoDrop®-based score to identify hemolysis in plasma and serum samples. Bioanalysis. 2014;6(9):1215-26.
69. Dypås L, Gutzkow K, Olsen A-K, Duale N. Molecular Portrait of Potential Attention Deficit/ Hyperactivity Disorder Candidate Genes and Regulating Micrornas Expression in Normal Human Developing Brain Tissues. Medical Research Archives. 2020;8(9).
70. Nolan T, Hands RE, Bustin SA. Quantification of mRNA using real-time RT-PCR. Nature Protocols. 2006;1(3):1559-82.
71. Schefe JH, Lehmann KE, Buschmann IR, Unger T, Funke-Kaiser H. Quantitative real-time RT-PCR data analysis: current concepts and the novel "gene expression's CT difference" formula. J Mol Med (Berl). 2006;84(11):901-10.
72. Vandesompele J, De Preter K, Pattyn F, Poppe B, Van Roy N, De Paepe A, et al. Genome Biology. 2002;3(7):research0034.1.
73. Šimkovic M, Träuble B. Robustness of statistical methods when measure is affected by ceiling and/or floor effect. PLOS ONE. 2019;14(8):e0220889.
74. Paul S, Reyes PR, Garza BS, Sharma A. MicroRNAs and Child Neuropsychiatric Disorders: A Brief Review. Neurochemical Research. 2020;45(2):232-40.
75. Kichukova TM, Popov NT, Ivanov HY, Vachev TI. Circulating microRNAs as a Novel Class of Potential Diagnostic Biomarkers in Neuropsychiatric Disorders. Folia Medica. 2016;57(3-4):159-72.
76. Wu LH, Peng M, Yu M, Zhao QL, Li C, Jin YT, et al. Circulating MicroRNA Let-7d in Attention-Deficit/Hyperactivity Disorder. NeuroMolecular Medicine. 2015;17(2):137-46.
77. Kandemir H, Erdal ME, Selek S, Ay Öİ, Karababa İF, Kandemir SB, et al. Evaluation of several micro RNA (miRNA) levels in children and adolescents with attention deficit hyperactivity disorder. Neuroscience Letters. 2014;580:158-62.
78. Cheng HH, Yi HS, Kim Y, Kroh EM, Chien JW, Eaton KD, et al. Plasma Processing Conditions Substantially Influence Circulating microRNA Biomarker Levels. PLoS ONE. 2013;8(6):e64795.
79. Vembadi A, Menachery A, Qasaimeh MA. Cell Cytometry: Review and Perspective on Biotechnological Advances. Frontiers in Bioengineering and Biotechnology. 2019;7.
80. Ravi, Vijayalaxmi, Gross C, Yao X, Xing L, Laur O, et al. Reversible Inhibition of PSD-95 mRNA Translation by miR-125a, FMRP Phosphorylation, and mGluR Signaling. Molecular Cell. 2011;42(5):673-88.
81. He J, Huang Z, He M, Liao J, Zhang Q, Wang S, et al. Circular RNA MAPK4 (circ-MAPK4) inhibits cell apoptosis via MAPK signaling pathway by sponging miR-125a-3p in gliomas. Molecular Cancer. 2020;19(1).
82. Zhang Y, Ueno Y, Liu XS, Buller B, Wang X, Chopp M, et al. The MicroRNA-17-92 Cluster Enhances Axonal Outgrowth in Embryonic Cortical Neurons. Journal of Neuroscience. 2013;33(16):6885-94.
83. Zhang X, Li Y, Qi P, Ma Z. Biology of MiR-17-92 Cluster and Its Progress in Lung Cancer. International Journal of Medical Sciences. 2018;15(13):1443-8.
84. Cao D, Jiang B, Zhang Y, Pang M. miR-125b-5p is A Promising Novel Plasma Biomarker for Alveolar Echinococcosis in Patients from the Southern Province of Qinghai. 2020.
85. Masucci GV, Cesano A, Hawtin R, Janetzki S, Zhang J, Kirsch I, et al. Validation of biomarkers to predict response to immunotherapy in cancer: Volume I — pre-analytical and analytical validation. Journal for ImmunoTherapy of Cancer. 2016;4(1).